EUROPEAN ORGANIZATION FOR NUCLEAR RESEARCH (CERN)

CERN-EP-2024-199
2024/07/31

CMS-HIG-21-004

Model-independent search for pair production of new bosons decaying into muons in proton-proton collisions at $\sqrt{s} = 13\,\text{TeV}$

The CMS Collaboration*

Abstract

The results of a model-independent search for the pair production of new bosons within a mass range of $0.21 < m < 60\,\text{GeV}$, are presented. This study utilizes events with a four-muon final state. We use two data sets, comprising $41.5\,\text{fb}^{-1}$ and $59.7\,\text{fb}^{-1}$ of proton-proton collisions at $\sqrt{s} = 13\,\text{TeV}$, recorded in 2017 and 2018 by the CMS experiment at the CERN LHC. The study of the 2018 data set includes a search for displaced signatures of a new boson within the proper decay length range of $0 < c\tau < 100\,\text{mm}$. Our results are combined with a previous CMS result, based on $35.9\,\text{fb}^{-1}$ of proton-proton collisions at $\sqrt{s} = 13\,\text{TeV}$ collected in 2016. No significant deviation from the expected background is observed. Results are presented in terms of a model-independent upper limit on the product of cross section, branching fraction, and acceptance. The findings are interpreted across various benchmark models, such as an axion-like particle model, a vector portal model, the next-to-minimal supersymmetric standard model, and a dark supersymmetric scenario, including those predicting a non-negligible proper decay length of the new boson. In all considered scenarios, substantial portions of the parameter space are excluded, expanding upon prior results.

Submitted to the Journal of High Energy Physics

*See Appendix A for the list of collaboration members

1 Introduction

Although the standard model (SM) [1–3] of particle physics provides a multitude of high-precision predictions consistent with decades of experimental results, it does not explain the existence of dark matter [4, 5]. Many models have been proposed that predict new bosons as dark matter candidates [6–8]. To date, no direct experimental evidence has materialized for particles beyond the SM (BSM), and in that context the idea of new bosons with non-negligible proper decay length [9] is of increasing interest. In this paper, we present a model-independent search for the pair production of a new boson that decays into a pair of oppositely charged muons. This can happen in proton-proton (pp) collisions as $\mathrm{pp} \to 2a + \mathrm{X} \to 4\mu + \mathrm{X}$, where a is the new neutral boson and X are possible spectator particles [10]. The new boson, a, can be produced via various "portals" connecting to a hidden sector, such as a Higgs boson, h, portal (either SM or non-SM) or a vector boson portal [8, 11, 12]. Here, the production vertices of dimuons, i.e., pairs of oppositely-charged muons in the final state, can be either prompt or displaced. The displaced case results from the decays of long-lived BSM bosons. This generic signature enables us to set a model-independent limit on the product of the new boson production cross section, branching fraction to muons squared, and acceptance. With this model-independent limit, further interpretation is possible in models with four muons in the final state.

We interpret the model-independent results in the context of several BSM benchmarks, including an axion-like particle (ALP) model [7, 13–16], a vector portal model with a dark scalar boson s_{D} [17–22], the next-to-minimal supersymmetric standard model (NMSSM) [6, 23–30], and supersymmetry (SUSY) models with hidden sectors (dark SUSY) [8, 22, 31]. In the ALP model [15], the SM-like Higgs boson, h, decays to the ALP, a, via $\mathrm{h} \to 2a$. The ALP then promptly decays into a dimuon. In the vector portal model, a massive dark vector boson Z_{D} decays to two new scalar bosons s_{D}, via $Z_{\mathrm{D}} \to s_{\mathrm{D}}\bar{s}_{\mathrm{D}}$, where we assume that the s_{D} is not self-conjugate, i.e., it is not equal to its antiparticle. The dark scalar boson s_{D} promptly decays to a dimuon. In the NMSSM, two of the three charge parity (CP) even, neutral Higgs bosons h_1 or h_2 (generically denoted $\mathrm{h}_{1,2}$) can decay to one of the two CP-odd neutral Higgs bosons a_1 via $\mathrm{h}_{1,2} \to 2a_1$. The CP-odd boson a_1 promptly decays to a dimuon. In the dark SUSY scenario, the breaking of a new $U(1)_{\mathrm{D}}$ symmetry gives rise to a massive dark photon γ_{D}. This dark photon can couple to SM photons via a small kinetic mixing parameter, ε. The proper decay length of the dark photon depends on its mass, $m_{\gamma_{\mathrm{D}}}$, and ε. We use a signal topology where an SM-like h decays to the lightest non-dark neutralino, n_1, via $\mathrm{h} \to 2\mathrm{n}_1$. These neutralinos then decay via $\mathrm{n}_1 \to \mathrm{n}_{\mathrm{D}} + \gamma_{\mathrm{D}}$, where n_{D} is an undetectable dark neutralino. The dark photon γ_{D} then decays to a dimuon. Figure 1 displays the Feynman diagrams of the benchmark signal models.

The search presented in this analysis improves upon the previous result published by the CMS Collaboration in Ref. [32]. Compared to this study, we add more data and add two new benchmark models, the ALP and vector portal models, and probe a larger mass range of the new, neutral boson a ($0.21 < m_a < 60\,\mathrm{GeV}$, compared to $0.25 < m_a < 8.5\,\mathrm{GeV}$ in Ref. [32]). Other searches at the LHC for $\mathrm{h} \to 2a$ include the 4e [33], 4μ [32, 34–37], 4τ [38, 39], 4ℓ [40–42], $4\ell/4\pi$ [33], $4\ell/8\ell$ [43], 4b [44, 45], 4γ [46], 2b 2τ [47, 48], 2μ 2τ [49, 50], and 6q [51] final states. This model-independent analysis considers both promptly-decaying and long-lived ($c\tau < 100\,\mathrm{mm}$) bosons, and it is complementary to those studies exploring ε in models with promptly-decaying [52, 53] and long-lived [54, 55] bosons that decay to a dimuon.

Two data sets are used for this analysis, which include data collected using multiple triggers in 2017 and 2018. These data sets correspond to integrated luminosities of 41.5 and $59.7\,\mathrm{fb}^{-1}$ of pp collisions at a center-of-mass energy of $\sqrt{s} = 13\,\mathrm{TeV}$, respectively. The results of the 2017 and 2018 data sets are first combined, corresponding to a total integrated luminosity of $101\,\mathrm{fb}^{-1}$.

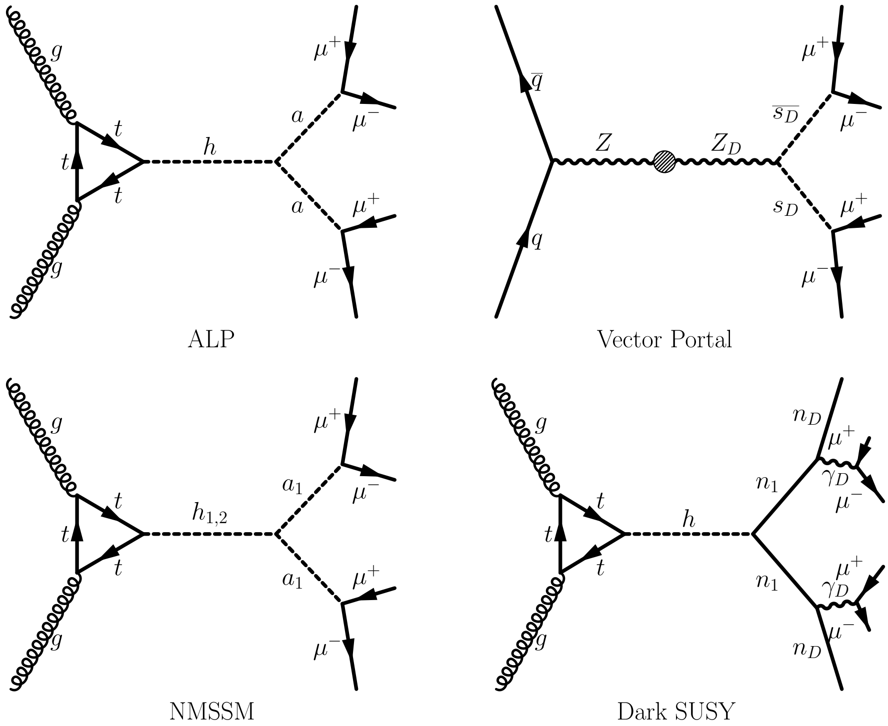

Figure 1: The Feynman diagrams of the benchmark signal models in the s-channel. Time moves from left to right.

We also combine these two data sets with a previously published analysis that examined the 2016 data-taking period [32], leading to results in the search mass range up to 9 GeV and corresponding to a total integrated luminosity of 137 fb^{-1}. Due to triggers using a primary vertex constraint in 2017, only 2018 data are used for the displaced signatures searches.

The CMS detector is improved in this data run with a new silicon pixel tracking detector [56] installed and commissioned in 2017 [57]. It features a larger detector volume with four layers in the barrel and three layers in the endcaps. Compared to the previous pixel detector, the innermost layer is positioned closer to the interaction point (IP) and the outermost layer is located farther from the IP. The new pixel detector can cope with a higher particle rate, improves impact parameter resolution, and increases the tracking efficiency. The performance of the hardware trigger algorithms for muons is also improved [58]. The analysis criteria are modified to accommodate the search in an extended model parameter space as compared to Ref. [32]. New benchmark models are added to further test the model independence and diversify the interpretation.

This paper is organized as follows: First, we discuss the layout and operation of the CMS detector in Section 2. Next, we review the simulation of signal samples in Section 3, event selection criteria in Section 4, and signal shape modeling in Section 5. We then present the processes of background estimation in Section 6, followed by a discussion of the systematic uncertainties in Section 7. Finally, we provide the results of this analysis in Section 8, which is followed by a brief summary in Section 9. Tabulated results are provided in the HEPData record for this analysis [59].

2 The CMS detector

The central feature of the CMS apparatus is a superconducting solenoid of 6 m internal diameter, providing a magnetic field of 3.8 T. Within the solenoid volume are a silicon pixel and strip tracker, a lead tungstate crystal electromagnetic calorimeter (ECAL), and a brass and scintillator hadron calorimeter (HCAL), each composed of a barrel and two endcap sections. Forward calorimeters extend the pseudorapidity coverage provided by the barrel and endcap detectors. Muons are reconstructed in gas-ionization detectors embedded in the steel flux-return yoke outside the solenoid.

Muons are measured in the pseudorapidity range $|\eta| < 2.4$, with detection planes made using three technologies: drift tubes, cathode strip chambers, and resistive plate chambers. The single muon trigger efficiency exceeds 90% over the full η range, and the efficiency to reconstruct and identify muons is greater than 96%. Matching muons to tracks measured in the silicon tracker results in a relative transverse momentum (p_{T}) resolution of 1% in the barrel and 3% in the endcaps, for muons with p_{T} up to 100 GeV. The p_{T} resolution in the barrel is better than 7% for muons with p_{T} up to 1 TeV [60].

Events of interest are selected using a two-tiered trigger system [61]. The first level (L1), is composed of custom hardware processors, and uses information from the calorimeters and muon detectors to select events at a rate of around 100 kHz within a fixed time interval of about 4 μs. The second level, known as the high-level trigger (HLT), consists of a farm of processors running a version of the full event reconstruction software optimized for fast processing. The HLT further reduces the event rate to around 1 kHz before the data are sent for permanent storage [61].

A more detailed description of the CMS detector, together with a definition of the coordinate system used and the relevant kinematic variables, can be found in Ref. [62].

3 Benchmark signal models

Simulated signal events are generated with Monte Carlo (MC) simulations and are used to determine the effect of the data selection criteria (described in Section 4) on the various signal models. In the ALP model, production of the SM-like h via gluon-gluon (gg) fusion and its subsequent decays are simulated at next-to-leading order (NLO) with the matrix-element generator MADGRAPH5_aMC@NLO 2.4.2 [63, 64]. The mass of the SM-like h is fixed to 125 GeV and masses between 0.5 and 30 GeV for the ALP are simulated. For the vector portal model, production of the spin-1 Z_{D} and its subsequent decays are simulated at NLO with MADGRAPH5_aMC@NLO 2.6.5. Masses of the Z_{D} between 85 and 200 GeV are simulated, thereby including the maximum Z_{D} production cross section [11]; the masses of the scalar boson s_{D} are simulated from 5 to 55 GeV depending on the kinematic constraints set by the Z_{D} mass.

For the NMSSM, production of the CP-even $\mathrm{h}_{1,2}$ via gg fusion and its decay to the CP-odd a_1 is carried out at leading order with PYTHIA 8.230 [65]. Since the $\mathrm{h}_{1,2}$ might not be the observed SM Higgs boson [66–68], mass values of $m_{\mathrm{h}_{1,2}}$ between 90 and 150 GeV are simulated. This range is motivated by constraints set by the relic density measurements from WMAP [69], Planck [70], and searches at LEP [71–76]. The mass of the boson a_1 is set to vary between 0.5 and 3 GeV as motivated in Ref. [77].

In the dark SUSY model, production of the SM-like Higgs boson via gg fusion and its decays are simulated at NLO with MADGRAPH5_aMC@NLO 2.4.2. The masses of the SM Higgs boson, the neutralino n_1, and the dark neutralino n_{D} are fixed to 125, 60, and 1 GeV, respectively. Dark photon masses m_{γ_D} are simulated between 0.25 and 58 GeV, and are set to exclusively decay to a pair of oppositely charged muons. Since the dark photon interacts weakly with SM particles, its decay width is negligible compared to the dimuon mass resolution.

Discussed in greater detail in Section 4, we consider displaced tracks and vertices for the case of long-lived mediators in the 2018 analysis only. This is because the 2017 data set lacks triggers that are comparable to those used in the 2018 analysis for displaced signatures. When considering muon displacement for the 2018 analysis, we model the displaced vertices in the lab frame via an exponential distribution with $c\tau_{\gamma_D}$ between 0 and 100 mm.

For all benchmark samples, pp collisions at 13 TeV are simulated using a set of parton distribution functions (PDFs) provided by NNPDF3.1 [78]. The parton shower, underlying event activity, and hadronization processes at the LHC are modeled with the MC event generator PYTHIA 8.230 using the CP5 tune [79]. Pileup (PU), or additional collisions, are added to these events, which are run through the full CMS detector simulation based on GEANT4 [80]. These events are then reconstructed with the same algorithms that are used for the data.

4 Event selection

Several triggers were used to collect the data used in this study, all exhibiting a total efficiency that exceeds 90% for all signal benchmarks described in Section 3. For the 2017 data set, we employ a double muon trigger with p_T thresholds of 23 and 12 GeV. Three additional triggers with lower p_T thresholds are implemented to further improve the trigger efficiency for potential signals: a double muon trigger requiring muons of the same sign, with p_T thresholds of 18 and 9 GeV, a triple muon trigger with p_T thresholds of 12, 5, and 5 GeV, and a triple tracker muon trigger with p_T thresholds of 12, 10, and 5 GeV. This last trigger requires "tracker muons" for which the tracker muon algorithm matches candidate muon segments from the tracker to segments from the innermost muon station [60].

The 2018 data set retains the last three triggers used in the 2017 data set but replaces the first trigger by one that is sensitive to displaced signatures. The so-called "double standalone" (SA) muon trigger requires at least two muons reconstructed using the muon detectors only [60], with a transverse momentum and pseudorapidity of $p_T > 23$ GeV and $|\eta| < 2$, respectively. This trigger was operated in 2018 and is used in the 2018 analysis. This double SA muon trigger does not rely on a primary vertex (PV) constraint for the track fit and is sensitive to both the prompt and displaced muons probed in this search. The PV is taken to be the vertex corresponding to the hard scattering location of the original pp collision, evaluated using tracking information alone [81]. There was no equivalent trigger in 2017, a study on 2017 data of the comparable double SA muon triggers available in 2018 either showed poor efficiencies for displaced muons in the pixel volume of the CMS experiment or negligible effective luminosities, thereby eliminating the possibility of investigating displaced track and vertex signatures in the 2017 analysis.

For both the 2017 and 2018 analyses, we require at least four offline reconstructed muons in each event. Among these muons, the 2017 analysis requires all muons to be reconstructed with the particle-flow (PF) algorithm [82], which performs a global fit that combines information from each subdetector, while the 2018 analysis requires at least three muons to be reconstructed with the PF algorithm and at most one SA muon reconstructed using only the information from the muon system. Selecting one possible SA muon in the 2018 analysis mitigates the efficiency lost for displaced muon reconstruction in the tracker by roughly 30%. Additional offline selection criteria are as follows: Each muon in the 2017 and 2018 analyses must have

$p_{\mathrm{T}} > 8\,\mathrm{GeV}$ and $|\eta| < 2.4$. For the 2017 analysis, we require at least two "high-p_{T} muons", i.e., muons with $p_{\mathrm{T}} > 13\,\mathrm{GeV}$. In the 2018 analysis, we require a higher threshold for these two "high-p_{T} muons", with $p_{\mathrm{T}} > 24\,\mathrm{GeV}$. For both the 2017 and 2018 analyses, we also require that these "high-p_{T} muons" are located in the region $|\eta| < 2$.

For both the 2017 and 2018 analyses the following selections are made: Any two oppositely charged muons in the event are paired as long as their invariant mass is below 60 GeV. The decay vertices of each dimuon in each event are reconstructed using the Kalman filtering (KF) technique [83], and only those vertices with a valid fitted vertex are retained. We then select the two dimuons closest in invariant mass. These two dimuons must not have any muons in common with each other. A dimuon that does not contain a high-p_{T} muon is labeled a low-p_{T} dimuon (denoted as $\mu\mu_2$), while the other dimuon, which includes at least one high-p_{T} muon, is called a high-p_{T} dimuon (denoted as $\mu\mu_1$). In the scenario where both dimuons contain a high-p_{T} muon, the dimuons are randomly labeled to prevent bias in the kinematic distributions. All single muons not included in the two dimuons are called orphan muons. No requirements are applied to the orphan muons. We require that each of the two dimuons contain at least one muon that has at least one valid hit in any of the layers of the pixel detector. This requirement ensures the selected dimuons originate from the signal bosons that decay in the pixel detectors.

To further ensure that the signal muons in each dimuon decay from the same boson, we require a limit on the Kalman-fitted dimuon vertex probability, $P_{\mu\mu}$. For the 2017 analysis, this level is set to 15%. As the dimuon transverse displacement (L_{xy}) and the opening angle of the two muons $\left(\Delta R = \sqrt{(\Delta\eta)^2 + (\Delta\phi)^2}\right)$ increases, the fitted vertex probability decreases. As the 2018 analysis considers displaced signals, we account for this difference by defining a probability threshold that is a function of L_{xy}, ΔR, and the number of SA muons, N_{SA}, and select valid fitted vertices based on the criterion $P_{\mu\mu} > P\left(L_{xy}, \Delta R, N_{\mathrm{SA}}\right)$.

The model independence of the results in this search is confirmed by verifying that the ratio of the full reconstruction efficiency ϵ_{Full} over the generator level acceptance α_{Gen} is independent of all signal benchmarks. The acceptance α_{Gen} is defined as the fraction of MC-generated signal events that pass the generator-level kinematic and geometric selection criteria. The parameter ϵ_{Full} is defined as the fraction of MC-generated events that pass the trigger and full event selection criteria. The valid-vertices criterion is particularly important, as this selection contributes to the overall uniformity of the distribution in $\epsilon_{\mathrm{Full}}/\alpha_{\mathrm{Gen}}$. The ratio $\epsilon_{\mathrm{Full}}/\alpha_{\mathrm{Gen}}$ is found to be insensitive to variations in all signal benchmark parameters: over all of the MC samples, an average value of 0.403 ± 0.001 (0.418 ± 0.001) for $\epsilon_{\mathrm{Full}}/\alpha_{\mathrm{Gen}}$ is obtained for the 2017 (2018) analysis, along with its statistical uncertainty.

Finally, we place a selection on the transverse displacement of $L_{xy} < 16\,\mathrm{cm}$ and on the longitudinal displacement of $L_z < 51.6\,\mathrm{cm}$. The upper bounds on L_{xy} and L_z correspond to the dimensions of the outermost layers of the CMS pixel system and define the volume in which the decay of a new boson can be probed by this analysis.

We also require that each dimuon is sufficiently isolated by having a total isolation sum of less than 2.3 GeV. This isolation sum, $\mathrm{Iso}_{\mu\mu} = \sum_{\mathrm{tracks}} p_{\mathrm{T}}(\mathrm{track})$, is calculated as the scalar sum of the transverse momenta of all reconstructed tracks with $p_{\mathrm{T}} > 0.5\,\mathrm{GeV}$ in the vicinity of the dimuon, i.e., within $\Delta R < 0.4$ and $|z_{\mathrm{track}} - z_{\mu\mu}| < 0.1\,\mathrm{cm}$. Here, z_{track} is defined as the z coordinate of the point of closest approach of the track to the primary vertex along the beam axis, while $z_{\mu\mu}$ is the z position of the vertex associated with the dimuon propagated back to the beamline along the dimuon direction vector. Tracks included in the dimuon reconstruction are excluded from the isolation calculation. Requiring $\mathrm{Iso}_{\mu\mu} < 2.3\,\mathrm{GeV}$ effectively removes about 72% of the quantum chromodynamic (QCD) background radiation. For a comprehensive and compact representation of all selection criteria, see Table 1.

Table 1: The event selection requirements for the 2017 and 2018 analyses. In the signal muon selection row, the particle-flow loose muons refer to those muons that have tracks in both the tracker and the muon system, which is contrasted with the standalone (SA) muon selection, which only requires tracks in the muon system.

Selection	Additional information	Requirement 2017	Requirement 2018
Signal muon candidates	All 4 signal muons	4 PF loose muons	$\geq$3 PF loose muons and $\leq$1 SA muon
p_T ($\|\eta\|$)	All 4 signal muons 2 signal muons	$p_T > 8$ GeV ($\|\eta\| < 2.4$) $p_T > 13$ GeV ($\|\eta\| < 2.0$)	$p_T > 8$ GeV ($\|\eta\| < 2.4$) $p_T > 24$ GeV ($\|\eta\| < 2.0$)
Invariant mass	Each dimuon	$m_{\mu\mu_{1,2}} < 60$ GeV	$m_{\mu\mu_{1,2}} < 60$ GeV
Fitted dimuon vertex probability	Each dimuon	$P_{\mu\mu_{1,2}} > 0.15$	$P_{\mu\mu_{1,2}} > P(L_{xy}, \Delta R, N_{SA})$
Dimuon isolation	Each dimuon	$\mathrm{Iso}_{\mu\mu_{1,2}} < 2.3$ GeV ($\Delta R < 0.4$)	$\mathrm{Iso}_{\mu\mu_{1,2}} < 2.3$ GeV ($\Delta R < 0.4$)
Fiducial volume	Each dimuon	—	$L_{xy} < 16.0$ cm $L_z < 51.6$ cm

5 Signal shape modeling and signal region definition

The target new boson is presumed to be weakly coupled to SM particles with a narrow width; therefore, the shape of the dimuon invariant mass distribution is fully determined by the detector resolution and final-state radiation (FSR) from the muons.

The signal region (SR), defined by the signal mass window in the two-dimensional (2D) plane of $m_{\mu\mu_1}$ and $m_{\mu\mu_2}$ is determined by fitting the prompt signal shape distributions of the MC signal samples with a double-sided Crystal Ball (CB) function (modified from [84] to include a tail on each side of the Gaussian function). The fitting results for the displaced signal show no significant difference within the statistical fluctuations. This composite function consists of a Gaussian core and two power-law tails. The sigma parameter of the CB function describes the width of the Gaussian fit to the signal and, consequently, the signal resolution. To set the mass window size across the signal mass phase space, we extract the sigma parameter from the mass fit for each simulated mass point and plot it as a function of the invariant dimuon mass. To create a continuous signal mass window, we use the values obtained by linearly interpolating the plotted data points.

Because the two dimuons originate from identical bosons, the signal mass window selection is motivated by the requirement of consistent invariant masses of the dimuons. This requirement is displayed in Equation (1) below,

$$|m_{\mu\mu_1} - m_{\mu\mu_2}| < W\big((m_{\mu\mu_1} + m_{\mu\mu_2})/2\big) \tag{1}$$

where W is a function of the dimuon invariant masses $m_{\mu\mu_1}$ and $m_{\mu\mu_2}$, and is based on the interpolation of the sigma parameters previously discussed. To determine the best signal significance, $S/\sqrt{S+B}$, where S is the signal and B is the expected background in the SR, thereby maximizing the discovery potential of this work, we examine the effect of four different signal efficiencies for prompt signals: 80%, 85%, 90%, and 95%.

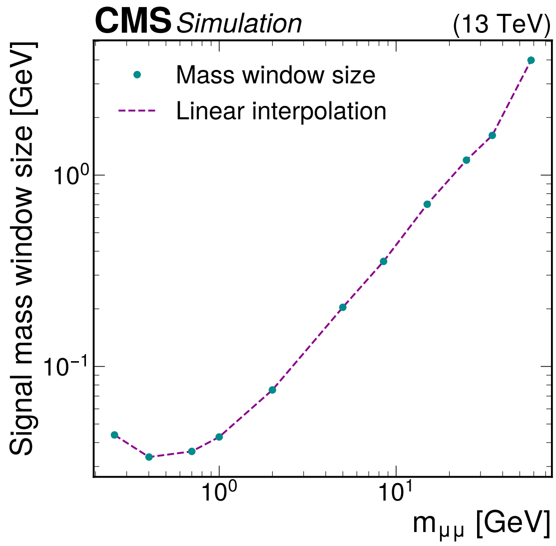

Figure 2: The mass window size as a function of invariant dimuon mass. It is derived from a Crystal Ball function fitting to MC signal events to contain 90% of events. The wider mass window size around $m_{\mu\mu} \lesssim 0.4\,\text{GeV}$ is due to the deteriorating mass resolution for near-collinear dimuons in the decays of low-mass bosons.

For all signal efficiencies chosen, the signal significance decreases as the dimuon mass increases. However, over the entire mass range probed, $0.21 < m_{\mu\mu} < 60\,\text{GeV}$, a signal mass window providing a 90% efficiency on signal events yielded the best signal significance. Figure 2 displays the size of the signal mass window as a function of invariant dimuon mass (green dots) with the line derived from linear interpolation (dashed, purple line). Thus, given the combination of the mass window size and placement in the $(m_{\mu\mu_1}, m_{\mu\mu_2})$ mass phase space, we achieve the optimal balance of signal significance and efficiency across the entire signal mass range, which we use to define the signal region (SR). This selection ultimately carves out the signal region in the 2D plane of $m_{\mu\mu_1}$ and $m_{\mu\mu_2}$, as illustrated by the dashed lines in Figs. 3 and 4.

6 Background estimation

To estimate the background, we first divide the mass range into regions below and above the Υ resonances and then split the range below the Υ further at the location of the J/ψ resonance. We exclude the mass ranges that contain the J/ψ (2.72–3.24 GeV) and the Υ (9–11 GeV) resonances. For the following discussion, we estimate the background in each region using fully data-driven methods based on data collected with the CMS detector.

6.1 Background below the Υ resonances

The major background contribution below the Υ resonances originates from QCD multijet processes. The QCD multijet background is dominated by events in which two b quarks decay to $2\mu + X$ or decay through low-mass meson resonances such as ω, ρ, ϕ, and $\psi(2S)$. A two-dimensional template $T(m_{\mu\mu_1}, m_{\mu\mu_2})$ is constructed in the plane of the two dimuon invariant masses to estimate the QCD background.

For both the 2017 and 2018 analyses the template is constructed over several steps. First, a

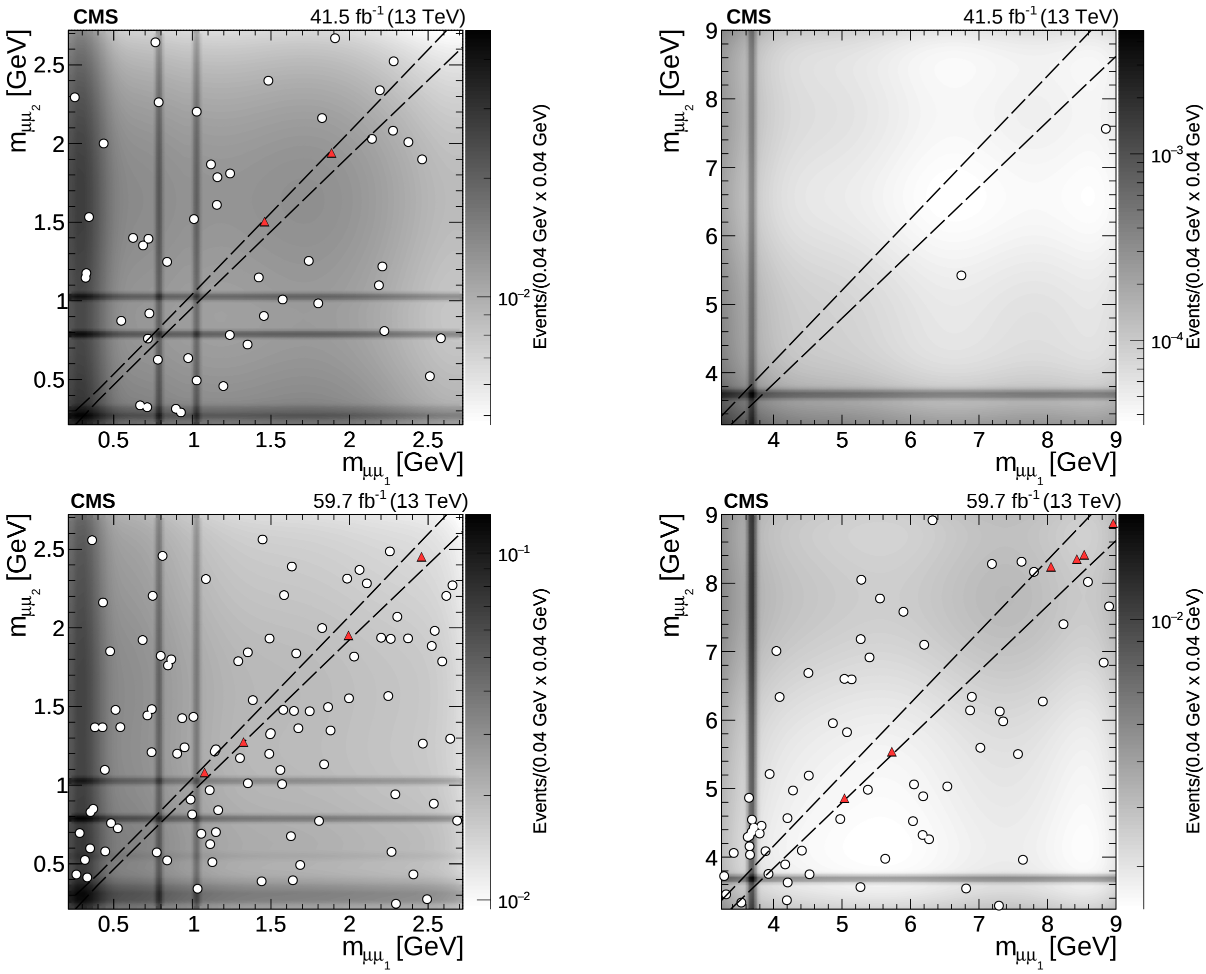

Figure 3: Two-dimensional distribution of the invariant masses $m_{\mu\mu_1}$ vs. $m_{\mu\mu_2}$ below (left) and above (right) the J/ψ resonance, for the 2017 (top row) and 2018 (bottom row) analyses. The greyscale heatmaps show the normalized QCD background templates, and the black vertical and horizontal bands correspond to the excluded regions around the η, $\omega(783)$, and $\phi(1020)$ resonances. The white dots represent data events that pass all selection criteria but fall outside the SR $m_{\mu\mu_1} \simeq m_{\mu\mu_2}$ (outlined by dashed lines), and the red triangles represent data events passing all selection criteria. As discussed in Section 6.1, the paucity of events in the CR for the 2017 analysis, particularly the region above J/ψ, is a result of the triggers selected for this data-taking period.

control sample is selected from the data. Events are required to have only one dimuon, at least one orphan muon, and pass the event selection criteria as applied to signal candidates, including the vertex probability and isolation selection on the only dimuon, the pixel hit requirements, and all of the signal triggers. The primary HLT used in this study is a high-p_{T}, double muon trigger; consequently, the three muon selection requirement must contain two high-p_{T} muons. If an event includes more than one orphan muon, the muon with the highest p_{T} is selected. Depending on where the high-p_{T} muons are, these events are separated into two categories. The first category corresponds to events where both muons in the only dimuon are high-pT muons, the mass of this dimuon system is used to model the $m_{\mu\mu_1}$ template. The second category contains events where the orphan muon is a high-p_{T} muon and the dimuon contains another high-p_{T} muon, the mass of the dimuon defines, in that case, the $m_{\mu\mu_2}$ variable. This procedure ensures that kinematic differences between signal events that have exactly two

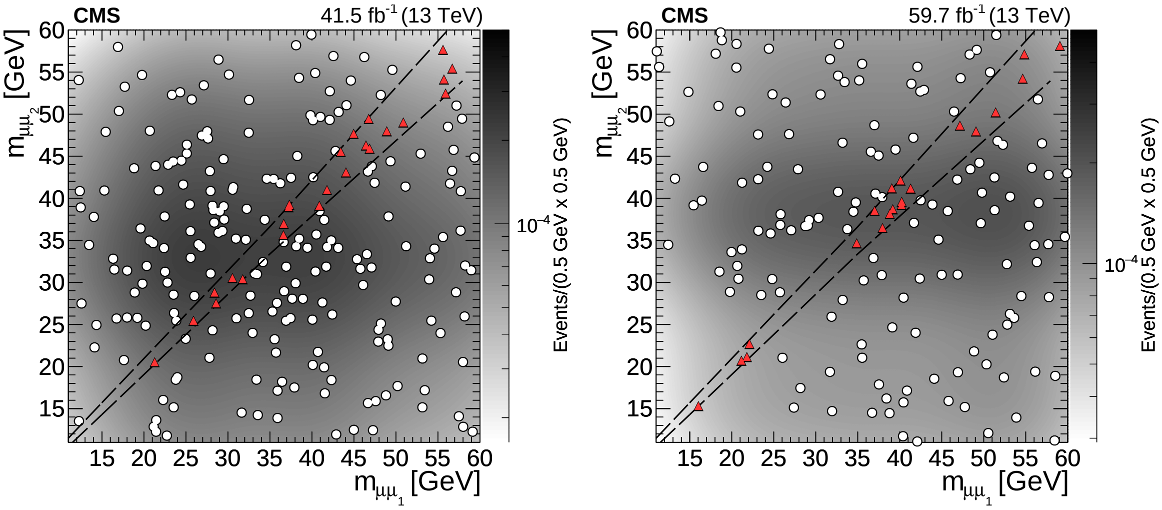

Figure 4: Two-dimensional distribution of the invariant masses $m_{\mu\mu_1}$ vs. $m_{\mu\mu_2}$ above the Υ resonances for the 2017 analysis (left) and the 2018 analysis (right). The greyscale heatmaps represent the normalized 2D probability density function of the background data. White dots represent data events that pass all selection criteria but fall outside the SR $m_{\mu\mu_1} \simeq m_{\mu\mu_2}$ (outlined by dashed lines), and the red triangles represent data events passing all selection criteria.

high-p_{T} dimuons or just one high-p_{T} dimuon are accounted for. For the 2018 analysis, the only dimuon in the event is required to have at most one SA muon, pass the selection on fitted vertex probability, and have at least one hit in the pixel system as explained in Section 4.

Next, two one-dimensional (1D) dimuon mass templates, $T_{\mathrm{I}}(m_{\mu\mu_1})$ and $T_{\mathrm{II}}(m_{\mu\mu_2})$, are obtained from the control sample. Each distribution is fitted with a function comprised of a Gaussian distribution for each light meson resonance and a set of sixth-degree Bernstein polynomials for the continuum background shape. The 2D template $T(m_{\mu\mu_1}, m_{\mu\mu_2})$ is obtained by taking the tensor product of the 1D templates, $T_{\mathrm{I}}(m_{\mu\mu_1}) \otimes T_{\mathrm{II}}(m_{\mu\mu_2})$.

Finally, the 2D template is normalized to unity in the dimuon-dimuon mass space for the region below and above the J/ψ resonance. The template is represented as a smooth function of the Cartesian product of $m_{\mu\mu_1}$ and $m_{\mu\mu_2}$, and is shown by the greyscale colormap in Fig. 3. Here, the SR defined in Section 4 is bounded by the dashed lines. The region of the mass space outside the SR represents the control region (CR) for the QCD background. The ratio between the integral of the template in the SR (I_{SR}) and the CR (I_{CR}), or $R = I_{\mathrm{SR}}/I_{\mathrm{CR}}$, is calculated for both the region below and above the J/ψ. For the 2017 analysis, the ratios in the region below and above the J/ψ are 0.046 and 0.096, respectively. Similarly, the ratios obtained for the 2018 analysis below and above the J/ψ are 0.044 and 0.093, respectively. The same figure also displays the events found in the data that pass all selection criteria except the consistent mass requirement, thus falling outside of the SR (represented as white dots).

For the 2017 (2018) analysis, there are in total 49 and 2 (98 and 66) events in the CR below and above the J/ψ resonance, respectively. We then estimate the number of background events in the SR below and above the J/ψ using the ratio R. In 2017, these values are $2.26 \pm 0.32\,(\mathrm{stat})$ and $0.19 \pm 0.14\,(\mathrm{stat})$, below and above the J/$\psi$, respectively. In 2018, these values are $4.34 \pm 0.44\,(\mathrm{stat})$ and $6.16 \pm 0.76\,(\mathrm{stat})$, below and above the J/$\psi$, respectively. The statistical uncertainty is calculated as the production of the ratio R with the square root of the number of CR events, or $R\sqrt{N_{\mathrm{CR}}}$. Since R effectively normalizes this value, it is also referred to as the normalization uncertainty. These values are also listed in Table 2 for convenience.

This method of estimating the QCD background is further validated by performing a Baker–Cousins (BC) χ^2 test [85] for the data in the CR and the constructed template. Both the 2D template $T(m_{\mu\mu_1}, m_{\mu\mu_2})$ and data events in the CR are projected into 1D histograms. The template integral is then scaled to the data entries. To calibrate the statistical test we randomly generated one million sets of pseudo-data based on the template. The χ^2 statistic of the BC test is calculated for each pseudo-data set and the template to obtain a distribution of the χ^2 values. The final calibrated p-value is obtained by calculating the χ^2 between the actual data and the template and quoting the fraction above the observed χ^2 statistic in the χ^2 distribution. Because we are considering a total mass phase space trifurcated by the J/ψ and Y resonances in two separate analyses (2017 and 2018), we perform the BC test for each of these regions and for both analyses. All p-values for $m_{\mu\mu_1}$ are contained in [0.043, 0.924], and all p-values for $m_{\mu\mu_2}$ are contained within [0.164, 0.889] for both the 2017 and 2018 analyses in the region below the Y resonances. Note that the lower range of p-values results from the paucity of background events in the 2017 data set. For a complete list of p-values, see Table 3.

6.2 Background above the Y resonances

Electroweak processes with two Z bosons, the $\mathrm{t\bar{t}}$ process, and the Drell–Yan (DY) process all contribute to the background above the Y resonances. Additionally, we consider the possibility of a radiated photon in the DY process that converts into a dimuon. Such an event could become a non-negligible background when a photon-converted muon is paired with an oppositely charged muon from the DY process. Most of these events, however, fail the requirement of consistent dimuon masses and reside in the CR. The limited number of such events in the data makes it difficult to model the shape of their distribution. To veto these events, the trailing mass $m^{\mathrm{alt}}_{\mathrm{trailing}}$ and trailing opening angle $\Delta R^{\mathrm{alt}}_{\mathrm{trailing}}$ from the alternative pairs are used. These variables are calculated as follows: once two dimuons are obtained from the normal muon pairing algorithm mentioned in Section 4, we alternatively pair these muons by taking one muon from each dimuon and pairing it with the oppositely charged muon in the other dimuon; the smaller invariant mass of alternative pairs is $m^{\mathrm{alt}}_{\mathrm{trailing}}$ and the smaller opening angle of two muons in alternative pairs is $\Delta R^{\mathrm{alt}}_{\mathrm{trailing}}$. This alternative pairing restores dimuons that come from the DY process and the radiated photon. Compared to the dimuon from the DY process, the photon-converted dimuon usually has a smaller invariant mass and a smaller opening angle between the two muons. A final requirement of $m^{\mathrm{alt}}_{\mathrm{trailing}} > 3\,\mathrm{GeV}$, or $\Delta R^{\mathrm{alt}}_{\mathrm{trailing}} > 0.2$, is used to veto these background events.

The selection of events with at most one SA muon in two dimuons also causes extra background that is hard to model with MC samples. For example, in the $\mathrm{t\bar{t}}$ process, one SA muon from the b quark decay can be paired with an oppositely charged muon from the W boson decay to form a dimuon. These dimuons are almost exclusively prompt. However, in the signal MC data, events that contain one SA muon often happen when the signal boson is displaced. To minimize the contamination of these background events in the actual data, we reject two-dimuon events containing one SA muon if both dimuons are prompt-like with $L_{xy} < 0.1\,\mathrm{cm}$. Also, SA muons in background events are usually caused by underlying event activity or punch-through effects. Such SA muons have fewer reconstructed muon segments in the muon detector than those from signal events. We require the SA muon to have at least two valid muon segments, which further rejects the background caused by the SA muon.

Because the template method [32] fails to describe the background above the Y resonances accurately, we use the kernel density estimate (KDE) method [86] to model the background in the region above the Y for both the 2017 and 2018 data sets. The KDE method is specifically chosen because it is a non-parametric method that operates on unbinned data, thereby eliminating the reliance on the input parameters typically used in the template method. The 2D probability density function (pdf) is built via the KDE method in two steps: First, the 1D pdf, using a Gaussian kernel with an adaptive bandwidth, is taken for both $m_{\mu\mu_1}$ and $m_{\mu\mu_2}$. The 2D pdf is then formed via the outer product of the pdfs for $m_{\mu\mu_1}$ and $m_{\mu\mu_2}$, i.e., $\hat{f}(m_{\mu\mu_1}, m_{\mu\mu_2}) = f_{\mathrm{I}}(m_{\mu\mu_1}) \otimes f_{\mathrm{II}}(m_{\mu\mu_2})$, where $f_{\mathrm{I,II}}(m_{\mu\mu})$ are the 1D pdfs. Figure 4 displays the 2D pdfs in the form of greyscale colormaps for the 2017 analysis (left) and the 2018 analysis (right). The dashed lines bound the SR, i.e., $\mathrm{SR}(m_{\mu\mu_1} \simeq m_{\mu\mu_2})$, and the white dots represent data events that fall outside this SR. The number of events in the CR above the Υ resonances is 212 and 143 for the 2017 and 2018 data sets, respectively. In the mass region above the Υ resonances, the ratio R is 0.085 (0.097) for the 2017 (2018) analyses. We then estimate the number of expected background events in the SR. For 2017, we expect 18.10 ± 1.23 (stat) events, and for 2018, we expect 13.81 ± 1.16 (stat) events. The systematic uncertainties are explained in detail in Section 7. For comparison across years and mass regions, these values and those from the low-mass regions are listed in Table 2.

Table 2: The number of observed events in the CR and the expected and observed number of events in the SR in the three mass regions considered in this analysis.

Region	Quantity	Year 2017	Year 2018
Below J/ψ	Obs. events in CR	49	98
	Exp. events in SR	2.26 ± 0.32 (stat) ± 0.14 (syst)	4.34 ± 0.44 (stat) ± 0.18 (syst)
	Obs. events in SR	2	4
Above J/ψ, Below Υ	Obs. events in CR	2	66
	Exp. events in SR	0.19 ± 0.14 (stat) ± 0.01 (syst)	6.16 ± 0.76 (stat) ± 0.09 (syst)
	Obs. events in SR	0	6
Above Υ	Obs. events in CR	212	143
	Exp. events in SR	18.10 ± 1.23 (stat) ± 4.49 (syst)	13.81 ± 1.16 (stat) ± 5.39 (syst)
	Obs. events in SR	24	20

To assess the goodness-of-fit of the pdfs produced via the KDE method, we perform the BC χ^2 test. Just like the template method, the 2D pdfs are separated into the 1D pdfs individually representing $m_{\mu\mu_1}$ and $m_{\mu\mu_2}$. The BC test is then performed on each 1D pdf in the same manner as described in Section 6.1, the results of which yield p-values in the range of [0.513, 0.974] for both invariant dimuon masses and both analyses. For completeness, we tabulate all p-values for both $m_{\mu\mu_1}$ and $m_{\mu\mu_2}$ in all three mass regions for both the 2017 and 2018 analyses in Table 3.

7 Systematic uncertainties

The leading source of experimental uncertainty in the signal prediction comes from the measurement of the integrated luminosity recorded by the CMS detector: during the 2017 (2018) data-taking period, this uncertainty was 2.3% [87] (2.5% [88]). Other experimental uncertainties include the uncertainty on the final signal efficiency at high PU conditions (2.3% in 2017 and 1.8% in 2018), the selection of consistent masses of the two dimuons (0.24% for both 2017 and 2018), the uncertainty in the signal trigger scale factor that corrects for different trigger efficiencies in the data and MC simulation (0.9% in 2017 and 0.6% in 2018), and the uncertainty in the modeling of the PU distribution (0.1% in 2017 and 0.05% in 2018). The uncertainty on the reconstruction of displaced tracks and vertices contributes to the total systematic uncertainty of the 2018 analysis only, and is quoted at 1.0%, with 0.5% contributing from each displaced

Table 3: Results of the Baker–Cousins χ^2 test for goodness-of-fit between the modeled background and the actual background events. For background below the Υ resonances, the 2D background templates are projected into one dimension, and the test is conducted, comparing background data and template values, yielding two p-values per region per data set. A similar procedure is followed for background above the Υ resonances: the 2D pdfs are projected into one dimension and the BC test is conducted, yielding two p-values for each dimuon invariant mass for both 2017 and 2018. Note that the low p-values for the mass region above J/ψ and below Υ for the 2017 data set result from the low number of background events in the data.

Region	p-value 2017		p-value 2018	
	$m_{\mu\mu_1}$	$m_{\mu\mu_2}$	$m_{\mu\mu_1}$	$m_{\mu\mu_2}$
Below J/ψ	0.333	0.889	0.186	0.164
Above J/ψ, below Υ	0.043	0.172	0.924	0.375
Above Υ	0.974	0.695	0.768	0.513

dimuon vertex fit [89]. The experimental uncertainties due to muon identification, dimuon isolation, and reconstruction of close muons in the tracker and the muon system can be found in Ref. [32], and are reproduced in Table 4. The theoretical uncertainties include the uncertainty in the PDFs, knowledge of the strong coupling constant α_S, the renormalization and factorization scales, and the production cross section of the Higgs boson and its branching fractions—all of these uncertainties can be found in Ref. [32] as well, and are also reproduced in Table 4.

We also consider systematic uncertainties for the estimated background. The dimuon isolation threshold described in Section 4 is varied by 5% around the threshold to achieve a total variation of 10%; the final number of expected background events in the SR is recomputed. The changes in the expected background events are quoted as a systematic uncertainty for the region below J/ψ (6.6% in 2017 and 4.1% in 2018), between J/ψ and Υ (5.9% in 2017 and 1.5% in 2018), and above Υ (1.2% in 2017 and 2.3% in 2018).

For the region above the Υ resonances, we determine a systematic uncertainty on the pdf background shape by examining the number of estimated events for two scenarios in which the number of CR events is reduced by half. This is accomplished by applying selections to the events in the CR, which reduce their number by 50% and comparing the estimated number of events in the SR resulting from these selections. For all selections placed, we first keep the SR constant and then impose two different linear inequalities that eliminate roughly half of the events in the CR, which are given by $0 \leq \zeta m_{\mu\mu_1} - \theta m_{\mu\mu_2}$ and $0 \geq \theta m_{\mu\mu_1} - \zeta m_{\mu\mu_2}$, where ζ and θ are arbitrary parameters chosen such that the desired 50% reduction of CR events is achieved.

We use these inequalities to exclude data to determine how the number of expected events in the SR changes, which provides a measure of the uncertainty on the background pdf shape. To produce this result, we consider two scenarios for both the 2017 and 2018 analyses: for the first scenario, we set the parameters $\zeta = 1.6$ and $\theta = 1$, and determine the number of expected events in the SR. For the second scenario, we swap the values of ζ and θ and again determine the number of events in the SR. The ratio of the SR and CR background yields, i.e., I_{SR}/I_{CR}, are computed and the expected background yields are compared to the nominal case where no selection is applied. The uncertainty on the background pdf shape is then taken as the largest percent difference, resulting in a 23.6% and 36.7% uncertainty for 2017 and 2018, respectively. Note that we do not include uncertainty on the background shape below the Υ resonances because this region was estimated using the template method. Table 4 presents all uncertainties used in this analysis.

Table 4: The systematic uncertainties for the 2017 and 2018 analyses, including the experimental uncertainties on the signal and background, as well as the theoretical uncertainties. The experimental uncertainties on the muon identification (ID), the dimuon isolation, and the reconstruction of close muons in both the tracker and the muon system have been reproduced from [32]. Additionally, all theoretical uncertainties have been reproduced from [32].

Source of uncertainty	Value 2017	Value 2018
Experimental signal uncertainties		
Integrated luminosity	2.3%	2.5%
Muon ID	$4 \times 0.6\%$	$4 \times 0.6\%$
Dimuon isolation	$2 \times 0.1\%$	$2 \times 0.1\%$
Reco. of close muons in tracker (signal mass $< 9\,\text{GeV}$)	$2 \times 1.2\%$	$2 \times 1.2\%$
Reco. of close muons in muon system (signal mass $< 9\,\text{GeV}$)	$2 \times 1.3\%$	$2 \times 1.3\%$
Muon HLT	0.9%	0.6%
Reconstruction of displaced track/vertex	—	$2 \times 0.5\%$
PU distribution	0.1%	0.05%
PU effect on signal efficiency	2.3%	1.8%
Dimuon mass consistency	0.24%	0.24%
Experimental background uncertainties below J/ψ (0.21–2.72 GeV)		
Normalization	14.2%	10.1%
Systematic	6.6%	4.1%
Experimental background uncertainties above J/ψ and below Υ (3.24–9 GeV)		
Normalization	73.5%	12.3%
Systematic	5.9%	1.5%
Experimental background uncertainties above Υ (11–60 GeV)		
Normalization	6.9%	8.4%
Systematic	1.2%	2.3%
Shape	23.6%	36.7%
Theoretical signal uncertainties		
PDF + α_S + QCD scales	8%	8%
Higgs cross-section and BR[a]	3.8%	3.8%
NNLO Higgs p_T re-weighting[a]	2%	2%

[a]Uncertainty is not used in the vector portal model.

During the 2017 and 2018 data-taking periods, an issue affecting the L1 trigger was detected [58, 90], affecting muon candidates' bunch crossing assignment. Here, the limited time resolution of the muon detectors could erroneously register a hit and fire the L1 trigger. To assess the impact of this L1 trigger issue, we re-weight the signal MC samples by the muon p_T and η and obtained a corrected value of ϵ_{Full}. From this re-weighting, we conclude that this L1 trigger issue has a negligible effect on ϵ_{Full}, causing an impact of less than 1%.

8 Results

After applying all selection criteria to the data sample, 26 (30) events are found in over the full mass range in SR for the 2017 (2018) analysis. Their distribution in the $m_{\mu\mu_1}$ and $m_{\mu\mu_2}$ phase space is shown in Figs. 3 and 4. This result is consistent with the sum of all background estimates described in Section 6. Model-independent observed upper limits at a 95% confidence level (CL) are set on the product of the production cross section of pairs of new bosons, the square of the branching fraction to dimuons, and the acceptance. Limits are set using the CL_s method [91, 92]. The test statistic used is based on the logarithm of the likelihood ratio [93]. The systematic uncertainties and their correlations have been accounted for by profiling the likelihood with respect to the nuisance parameters for each value of the signal strength. The following results have been determined using the CMS statistical analysis tool COMBINE [94].

The limit is shown as a function of m_a in Fig. 5 over the range $0.21 < m_a < 60$ GeV for the 2017 and 2018 analyses (top left and top right, respectively), for the combined 2017 and 2018 data set over the range $0.21 < m_a < 60$ GeV (bottom left), and for the combined 2016, 2017, and 2018 data set over the range $0.21 < m_a < 9$ GeV (bottom right), where the analysis presented in Ref. [32] provides the input data for the 2016 data set. Overall, the limit for the 2018 data set, the combination of the 2017 and 2018 data sets, and the combination of the 2016, 2017, and 2018 analyses varies between 0.049 and 0.247 fb for the model-independent interpretation. We now interpret this result in the context of the signal benchmark models.

For the ALP scenario, the model-independent limit in Fig. 5 can be used to set the limit on the ratio of the effective coupling between the ALP and the SM Higgs boson, C_{ah}^{eff}, and the square of the new-physics energy scale, Λ, or $C_{ah}^{\text{eff}}/\Lambda^2$. The partial width of the Higgs boson decay to two ALPs can be found in Ref. [15]. We assume the Higgs boson mass is 125 GeV, the partial width of Higgs boson decay to SM particles is 4.1 MeV, the production cross section of the SM H via gg fusion at the LHC is 48.93 pb at a center-of-mass energy of 13 TeV [95], the vacuum expectation value of the Higgs field is 246 GeV, and the branching fraction of the ALP to muons is 100% (or 10%). The observed 95% CL upper limit on $C_{ah}^{\text{eff}}/\Lambda^2$ as a function of the ALP mass m_a is shown in Fig. 6 (left). Through this analysis, we achieve further reach and greater sensitivity than Run 1 LHC searches [38, 96, 97] (summarized in Ref. [15]). Similarly, with different choices of $C_{ah}^{\text{eff}}/\Lambda^2$ ($1\,\text{TeV}^{-2}$, $0.1\,\text{TeV}^{-2}$ and $0.01\,\text{TeV}^{-2}$), and a decay width of the ALP to leptons as presented in Ref. [15], we set limits on the ratio of the effective coupling between the ALP and SM leptons, C_{ll}^{eff}, to the new-physics energy scale, or $C_{ll}^{\text{eff}}/\Lambda$, as shown in Fig. 6 (right). The limit on $C_{ll}^{\text{eff}}/\Lambda$ depends directly on the value assumed for the total ALP width. We fix the ALP total width to a constant reference point of 10^{-5} GeV for all mass points.

For the vector portal benchmark model, we set a 95% CL upper limit on the product of the production cross section of the Z_D, the branching fraction of the decay of Z_D to s_D and $\bar{s}_D$, and the squared branching fraction of the decay of s_D to two oppositely charged muons: $\sigma(\text{pp} \to Z_D)\mathcal{B}(Z_D \to s_D\bar{s}_D)\mathcal{B}^2(s_D \to 2\mu)$ as a function of the dark scalar mass m_{s_D} and the dark vector boson mass m_{Z_D}. This limit is subsequently translated to the limit on the product of the square of the kinetic mixing parameter, ε^2, times the branching fraction of the decay of Z_D to a pair of dark scalar bosons s_D, times the squared branching fraction of the decay of the s_D to a dimuon: $\varepsilon^2\mathcal{B}(Z_D \to s_D\bar{s}_D)\mathcal{B}^2(s_D \to 2\mu)$. This limit, for various m_{s_D} and m_{Z_D}, is shown in Fig. 7.

For the NMSSM scenario, the 95% CL observed upper limits are derived for $\sigma(\text{pp} \to \text{h}_{1,2} \to 2a_1)\mathcal{B}^2(a_1 \to 2\mu)$ as a function of m_{a_1} with $m_{\text{h}_1} = 90$ GeV (Fig. 8 left) and $m_{\text{h}_1} = 125$ GeV (Fig. 8 middle), with m_{h_2} fixed at 125 GeV; and $m_{\text{h}_2} = 150$ GeV (Fig. 8 right) with m_{h_1} fixed at 125 GeV. It is assumed that all contributions come from either h_1 or h_2; there is no case in which both h_1 and h_2 decay to the a_1.

For the dark SUSY scenario, a 95% CL observed upper limit is set on the product of the h production cross section and the branching fractions of the h decay to a pair of dark photons. The limit set by this experimental search is presented in Fig. 9 as areas excluded in a two-dimensional plane of ε and m_{γ_D}. Here, the Higgs boson mass is taken to be 125 GeV, and the production cross section of the Higgs boson via gg fusion at the LHC is 48.93 pb at 13 TeV [95].

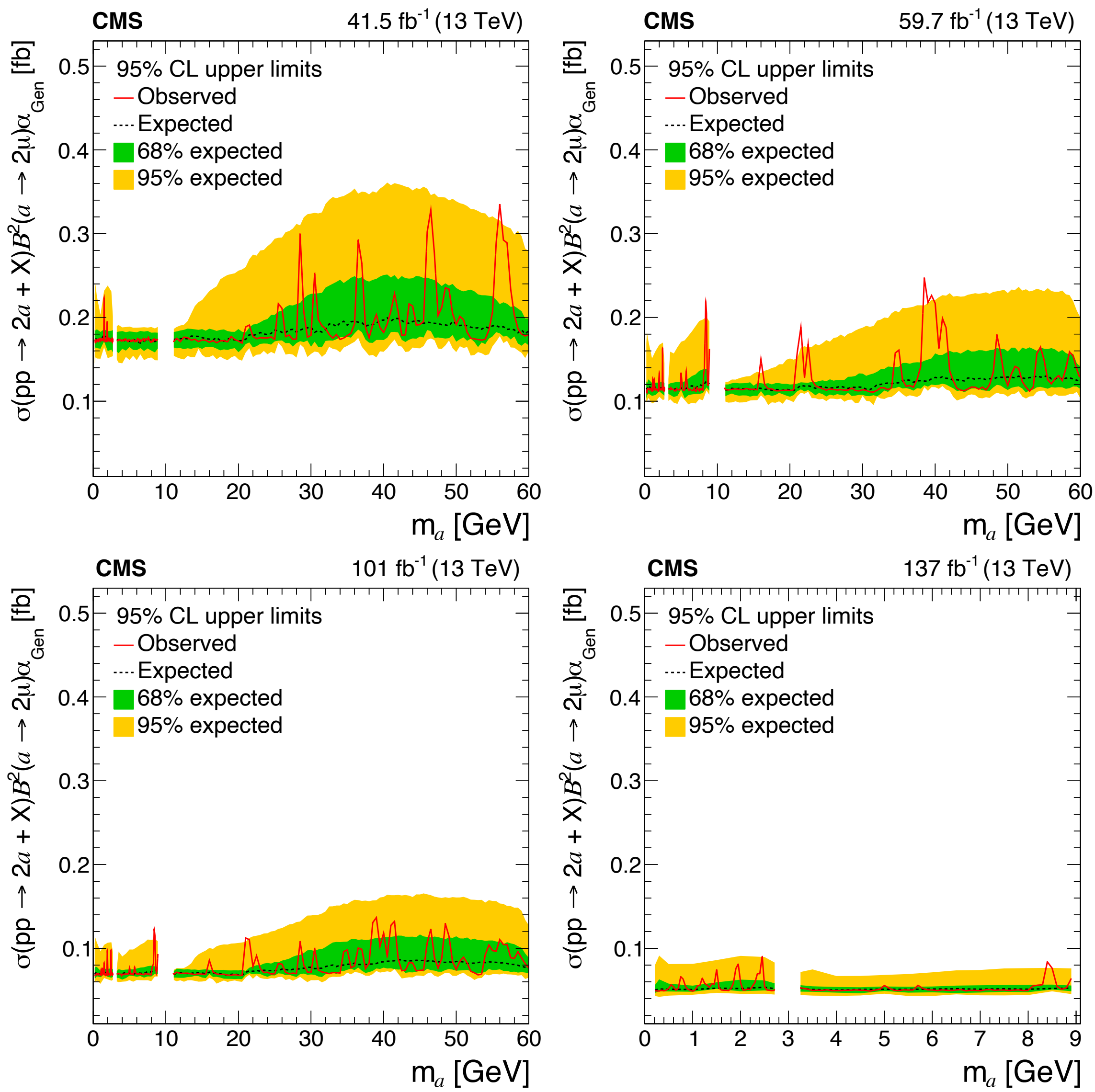

Figure 5: The model-independent 95% CL expected and observed upper limits set on $\sigma(pp \to 2a + X)\mathcal{B}^2(a \to 2\mu)\alpha_{Gen}$ over the range $0.21 < m_a < 60\,GeV$ for the 2017 and 2018 analyses (top left and top right, respectively), over the range $0.21 < m_a < 60\,GeV$ for the combined 2017 and 2018 analyses (bottom left), and over the range $0.21 < m_a < 9\,GeV$ for the combined 2016, 2017, and 2018 analyses (bottom right). Mass ranges that overlap with J/ψ and Υ resonances are excluded from the search.

For this search, limits are shown for the branching fraction of the h decay to two dark photons in the range 0.05–10%. The kinetic mixing parameter, ε, the mass of the dark photon m_{γ_D}, and the proper decay length of the dark photon $c\tau_{\gamma_D}$ are related via an analytic function that is solely dependent on the dark photon mass [98]. The proper decay length of the dark photon is allowed to vary from 0 to 100 mm and m_{γ_D} can range from 0.25 to 58 GeV. With the extended ranges in dimuon mass (0.21–60 GeV), this analysis excludes a previously unexplored area in the parameter space of ε and m_{γ_D} compared to the previous model-independent search (0.25–8.5 GeV) [32].

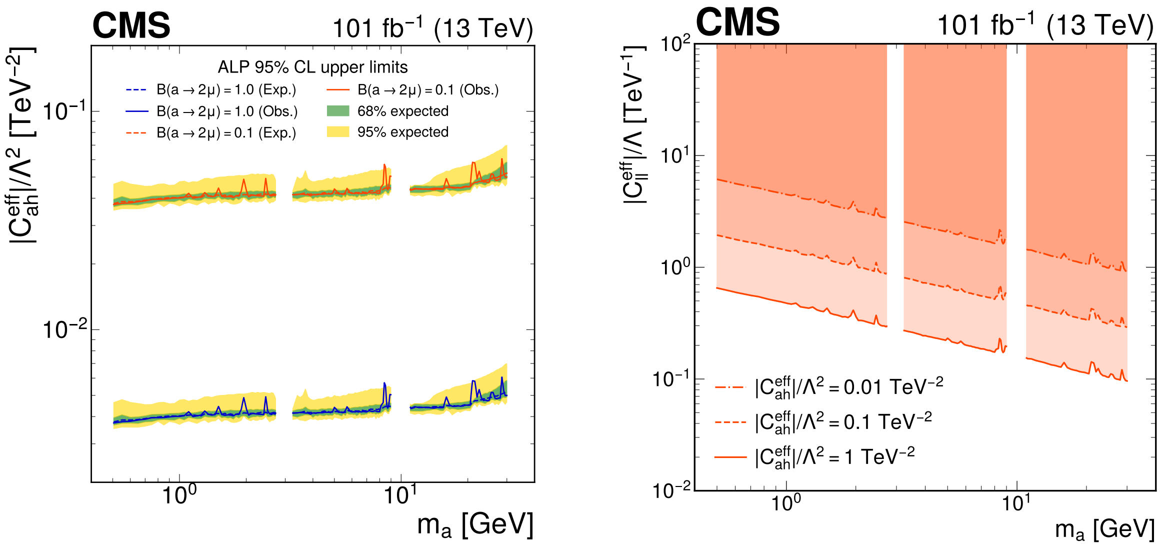

Figure 6: Left: The 95% CL observed upper limits on the effective coupling $C^{\rm eff}_{ah}/\Lambda^2$ of the ALP to the SM Higgs assuming the branching fraction of the ALP to muons is 1 (blue) and 0.1 (orange), for both the expected (dashed) and observed (solid) limits. Right: The 95% CL observed upper limits on the effective coupling $C^{\rm eff}_{ll}/\Lambda$ of the ALP to the SM leptons. The orange shaded region represents the parameter space excluded by this search under three choices of $C^{\rm eff}_{ah}/\Lambda^2$: 1 TeV^{-2} (solid), 0.1 TeV^{-2} (dashed), and 0.01 TeV^{-2} (dotted).

9 Summary

A search for pairs of new bosons a that subsequently decay to pairs of oppositely charged muons is presented. This search is performed using data samples collected by the CMS experiment in 2017 and 2018, corresponding to 41.5 fb^{-1} for the prompt signal in 2017 and 59.7 fb^{-1} for both the prompt and displaced signals in 2018, for proton-proton collisions at $\sqrt{s} = 13$ TeV. The results are also combined with a similar analysis performed by the CMS Collaboration [32], which analyzed a smaller data set collected in 2016 corresponding to 35.9 fb^{-1} of proton-proton collisions at $\sqrt{s} = 13$ TeV. Additionally, both the mass range of the boson a and the maximum possible displacement of its decay vertex are extended compared to the previous version of this analysis. The distribution of events in the signal region is consistent with standard model expectations. Model-independent 95% confidence level upper limits on the product of the production cross section of pairs of new bosons, the square of the branching fraction to dimuons, and the acceptance are set over the mass range $0.21 < m_a < 60$ GeV and are found to vary between 0.049 and 0.247 fb. These model-independent limits are then interpreted in the context of an axion-like particle model, a vector portal model, a next-to-minimal supersymmetric standard model, and a dark supersymmetry scenario with non-negligible boson proper decay length of up to $c\tau = 100$ mm.

Acknowledgments

We congratulate our colleagues in the CERN accelerator departments for the excellent performance of the LHC and thank the technical and administrative staffs at CERN and at other CMS institutes for their contributions to the success of the CMS effort. In addition, we gratefully acknowledge the computing centers and personnel of the Worldwide LHC Computing

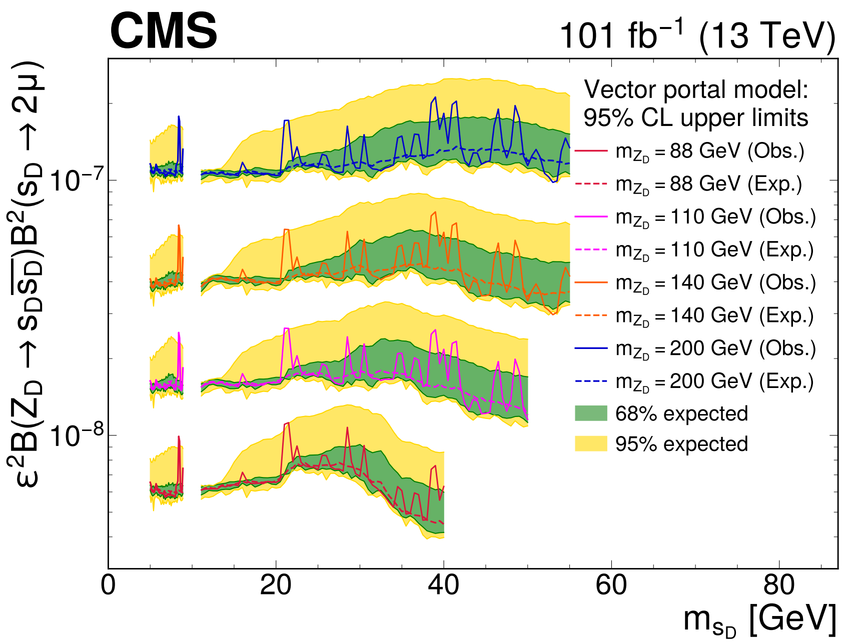

Figure 7: The 95% CL observed upper limits on $\varepsilon^2\mathcal{B}(Z_D \to s_D\bar{s}_D)\mathcal{B}^2(s_D \to 2\mu)$ for the vector portal model as a function of the dark scalar mass m_{s_D} and dark vector boson mass m_{Z_D}. Because the model-independent limits are calculated only up to a dimuon mass of 60 GeV, the s_D mass considered for these limits is below 60 GeV.

Grid and other centers for delivering so effectively the computing infrastructure essential to our analyses. Finally, we acknowledge the enduring support for the construction and operation of the LHC, the CMS detector, and the supporting computing infrastructure provided by the following funding agencies: SC (Armenia), BMBWF and FWF (Austria); FNRS and FWO (Belgium); CNPq, CAPES, FAPERJ, FAPERGS, and FAPESP (Brazil); MES and BNSF (Bulgaria); CERN; CAS, MoST, and NSFC (China); MINCIENCIAS (Colombia); MSES and CSF (Croatia); RIF (Cyprus); SENESCYT (Ecuador); ERC PRG, RVTT3 and MoER TK202 (Estonia); Academy of Finland, MEC, and HIP (Finland); CEA and CNRS/IN2P3 (France); SRNSF (Georgia); BMBF, DFG, and HGF (Germany); GSRI (Greece); NKFIH (Hungary); DAE and DST (India); IPM (Iran); SFI (Ireland); INFN (Italy); MSIP and NRF (Republic of Korea); MES (Latvia); LMTLT (Lithuania); MOE and UM (Malaysia); BUAP, CINVESTAV, CONACYT, LNS, SEP, and UASLP-FAI (Mexico); MOS (Montenegro); MBIE (New Zealand); PAEC (Pakistan); MES and NSC (Poland); FCT (Portugal); MESTD (Serbia); MCIN/AEI and PCTI (Spain); MOSTR (Sri Lanka); Swiss Funding Agencies (Switzerland); MST (Taipei); MHESI and NSTDA (Thailand); TUBITAK and TENMAK (Turkey); NASU (Ukraine); STFC (United Kingdom); DOE and NSF (USA).

Individuals have received support from the Marie-Curie program and the European Research Council and Horizon 2020 Grant, contract Nos. 675440, 724704, 752730, 758316, 765710, 824093, 101115353, 101002207, and COST Action CA16108 (European Union); the Leventis Foundation; the Alfred P. Sloan Foundation; the Alexander von Humboldt Foundation; the Science Committee, project no. 22rl-037 (Armenia); the Belgian Federal Science Policy Office; the Fonds pour la Formation à la Recherche dans l'Industrie et dans l'Agriculture (FRIA-Belgium); the F.R.S.-FNRS and FWO (Belgium) under the "Excellence of Science – EOS" – be.h project n. 30820817; the Beijing Municipal Science & Technology Commission, No. Z191100007219010

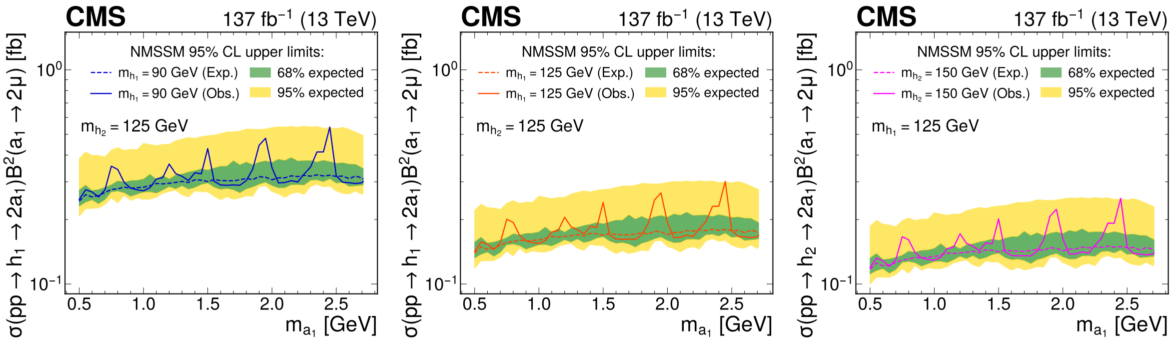

Figure 8: The 95% CL observed upper limits for $\sigma(\mathrm{pp} \to \mathrm{h}_{1,2} \to 2a_1)\mathcal{B}^2(a_1 \to 2\mu)$ for the NMSSM as a function of m_{a_1} for three choices of $m_{\mathrm{h}_{1,2}}$. The left and middle plots have m_{h_2} fixed to 125 GeV and the right plot has m_{h_1} fixed to 125 GeV. The data presented here reflect the results of the 2017 and 2018 data sets combined with the previously published results of the 2016 data set in [32].

and Fundamental Research Funds for the Central Universities (China); the Ministry of Education, Youth and Sports (MEYS) of the Czech Republic; the Shota Rustaveli National Science Foundation, grant FR-22-985 (Georgia); the Deutsche Forschungsgemeinschaft (DFG), among others, under Germany's Excellence Strategy – EXC 2121 "Quantum Universe" – 390833306, and under project number 400140256 - GRK2497; the Hellenic Foundation for Research and Innovation (HFRI), Project Number 2288 (Greece); the Hungarian Academy of Sciences, the New National Excellence Program - ÚNKP, the NKFIH research grants K 131991, K 133046, K 138136, K 143460, K 143477, K 146913, K 146914, K 147048, 2020-2.2.1-ED-2021-00181, and TKP2021-NKTA-64 (Hungary); the Council of Science and Industrial Research, India; ICSC – National Research Center for High Performance Computing, Big Data and Quantum Computing and FAIR – Future Artificial Intelligence Research, funded by the NextGenerationEU program (Italy); the Latvian Council of Science; the Ministry of Education and Science, project no. 2022/WK/14, and the National Science Center, contracts Opus 2021/41/B/ST2/01369 and 2021/43/B/ST2/01552 (Poland); the Fundação para a Ciência e a Tecnologia, grant CEECIND/01334/2018 (Portugal); the National Priorities Research Program by Qatar National Research Fund; MCIN/AEI/10.13039/501100011033, ERDF "a way of making Europe", and the Programa Estatal de Fomento de la Investigación Científica y Técnica de Excelencia María de Maeztu, grant MDM-2017-0765 and Programa Severo Ochoa del Principado de Asturias (Spain); the Chulalongkorn Academic into Its 2nd Century Project Advancement Project, and the National Science, Research and Innovation Fund via the Program Management Unit for Human Resources & Institutional Development, Research and Innovation, grant B39G670016 (Thailand); the Kavli Foundation; the Nvidia Corporation; the SuperMicro Corporation; the Welch Foundation, contract C-1845; and the Weston Havens Foundation (USA).

References

[1] F. Englert and R. Brout, "Broken symmetry and the mass of gauge vector mesons", *Phys. Rev. Lett.* **13** (1964) 321, doi:10.1103/PhysRevLett.13.321.

[2] P. W. Higgs, "Broken symmetries and the masses of gauge bosons", *Phys. Rev. Lett.* **13** (1964) 508, doi:10.1103/PhysRevLett.13.508.

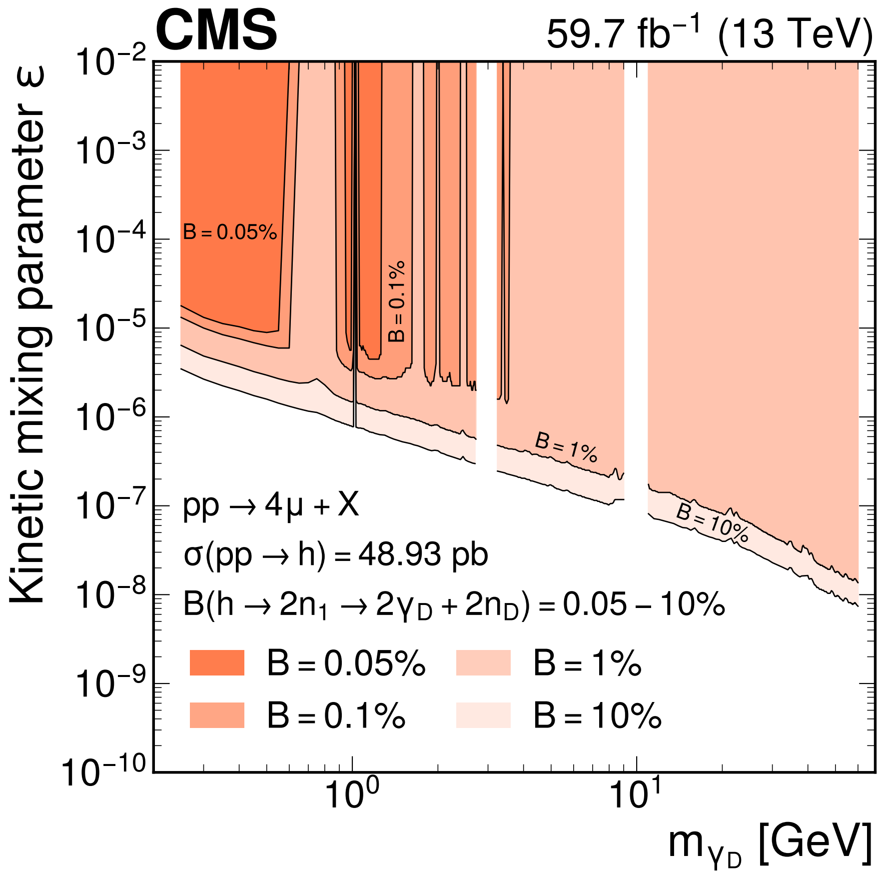

Figure 9: The 95% CL observed upper limits (black solid curves) from this search as interpreted in the dark SUSY scenario for the process $\mathrm{pp} \to \mathrm{h} \to 2\mathrm{n}_1 \to 2\gamma_\mathrm{D} + 2\mathrm{n}_\mathrm{D} \to 4\mu + \mathrm{X}$, with $m_{\mathrm{n}_1} = 60\,\mathrm{GeV}$ and $m_{\mathrm{n}_\mathrm{D}} = 1\,\mathrm{GeV}$. The limits are presented in the plane of ε and m_{γ_D}. The color gradient represents different branching fraction assumptions for $\mathcal{B}(\mathrm{h} \to 2\mathrm{n}_1 \to 2\gamma_\mathrm{D} + 2\mathrm{n}_\mathrm{D})$, ranging from dark orange (0.05%) to light orange (10%). The degradation of the limit around 1 GeV is attributed to the drop in the dimuon branching fraction $\mathcal{B}(\gamma_\mathrm{D} \to 2\mu)$ due to the dimuon resonance of the ϕ meson [98].

[3] G. S. Guralnik, C. R. Hagen, and T. W. B. Kibble, “Global conservation laws and massless particles”, *Phys. Rev. Lett.* **13** (1964) 585, doi:10.1103/PhysRevLett.13.585.

[4] V. Trimble, “Existence and nature of dark matter in the universe”, *Ann. Rev. Astron. Astrophys.* **25** (1987) 425, doi:10.1146/annurev.aa.25.090187.002233.

[5] G. Bertone and D. Hooper, “History of dark matter”, *Rev. Mod. Phys.* **90** (2018) 045002, doi:10.1103/RevModPhys.90.045002, arXiv:1605.04909.

[6] M. Maniatis, “The next-to-minimal supersymmetric extension of the standard model reviewed”, *Int. J. Mod. Phys. A* **25** (2010) 3505, doi:10.1142/S0217751X10049827, arXiv:0906.0777.

[7] L. D. Duffy and K. van Bibber, “Axions as dark matter particles”, *New J. Phys.* **11** (2009) 105008, doi:10.1088/1367-2630/11/10/105008, arXiv:0904.3346.

[8] N. Arkani-Hamed, D. P. Finkbeiner, T. R. Slatyer, and N. Weiner, "A theory of dark matter", *Phys. Rev. D* **79** (2009) 015014, doi:10.1103/PhysRevD.79.015014, arXiv:0810.0713.

[9] L. Lee, C. Ohm, A. Soffer, and T.-T. Yu, "Collider searches for long-lived particles beyond the standard model", *Prog. Part. Nucl. Phys.* **106** (2019) 210, doi:10.1016/j.ppnp.2019.02.006, arXiv:1810.12602.

[10] A. Belyaev et al., "LHC discovery potential of the lightest nmssm higgs boson in the $h_1 \to a_1 a_1 \to 4\mu$ channel", *Phys. Rev. D* **81** (2010) 075021, doi:10.1103/PhysRevD.81.075021, arXiv:1002.1956.

[11] M. Rahmani, "Construction and testing of large-area GEM detectors for the forward muon endcap upgrade of the CMS experiment and vector-portal search for dark matter particles with dimuon pairs at $\sqrt{s} = 13\,\text{TeV}$". PhD thesis, Florida Institute of Technology, 2022.

[12] D. Curtin, R. Essig, S. Gori, and J. Shelton, "Illuminating dark photons with high-energy colliders", *JHEP* **02** (2015) 157, doi:10.1007/JHEP02(2015)157, arXiv:1412.0018.

[13] E. Armengaud et al., "Axion searches with the EDELWEISS-II experiment", *JCAP* **11** (2013) 067, doi:10.1088/1475-7516/2013/11/067, arXiv:1307.1488.

[14] G. G. Raffelt, "Astrophysical axion bounds", *Lect. Notes Phys.* **741** (2008) 51, doi:10.1007/978-3-540-73518-2_3, arXiv:hep-ph/0611350.

[15] M. Bauer, M. Neubert, and A. Thamm, "Collider probes of axion-like particles", *JHEP* **12** (2017) 044, doi:10.1007/JHEP12(2017)044, arXiv:1708.00443.

[16] S. Weinberg, "A new light boson?", *Phys. Rev. Lett.* **40** (1978) 223, doi:10.1103/PhysRevLett.40.223.

[17] M. R. Buckley, D. Feld, and D. Goncalves, "Scalar simplified models for dark matter", *Phys. Rev. D* **91** (2015) 015017, doi:10.1103/PhysRevD.91.015017, arXiv:1410.6497.

[18] J. D. Wells, "How to find a hidden world at the Large Hadron Collider", in *Perspectives on LHC Physics*, G. Kane and A. Pierce, eds., p. 283. 2008. arXiv:0803.1243. doi:10.1142/6686.

[19] J. A. Aguilar-Saavedra, J. A. Casas, J. Quilis, and R. Ruiz de Austri, "Multilepton dark matter signals", *JHEP* **04** (2020) 069, doi:10.1007/JHEP04(2020)069, arXiv:1911.03486.

[20] D. Abercrombie et al., "Dark matter benchmark models for early LHC Run-2 searches: report of the ATLAS/CMS dark matter forum", *Phys. Dark Univ.* **27** (2020) 100371, doi:10.1016/j.dark.2019.100371, arXiv:1507.00966.

[21] F. Bishara, R. Contino, and J. Rojo, "Higgs pair production in vector-boson fusion at the LHC and beyond", *Eur. Phys. J. C* **77** (2017) 481, doi:10.1140/epjc/s10052-017-5037-9, arXiv:1611.03860.

[22] M. Baumgart et al., "Non-Abelian dark sectors and their collider signatures", *JHEP* **04** (2009) 014, doi:10.1088/1126-6708/2009/04/014, arXiv:0901.0283.

[23] P. Fayet, "Supergauge invariant extension of the Higgs mechanism and a model for the electron and its neutrino", *Nucl. Phys. B* **90** (1975) 104, doi:10.1016/0550-3213(75)90636-7.

[24] R. K. Kaul and P. Majumdar, "Cancellation of quadratically divergent mass corrections in globally supersymmetric spontaneously broken gauge theories", *Nucl. Phys. B* **199** (1982) 36, doi:10.1016/0550-3213(82)90565-X.

[25] R. Barbieri, S. Ferrara, and C. A. Savoy, "Gauge models with spontaneously broken local supersymmetry", *Phys. Lett. B* **119** (1982) 343, doi:10.1016/0370-2693(82)90685-2.

[26] H. P. Nilles, M. Srednicki, and D. Wyler, "Weak interaction breakdown induced by supergravity", *Phys. Lett. B* **120** (1983) 346, doi:10.1016/0370-2693(83)90460-4.

[27] J. M. Frere, D. R. T. Jones, and S. Raby, "Fermion masses and induction of the weak scale by supergravity", *Nucl. Phys. B* **222** (1983) 11, doi:10.1016/0550-3213(83)90606-5.

[28] J. P. Derendinger and C. A. Savoy, "Quantum effects and SU(2) x U(1) breaking in supergravity gauge theories", *Nucl. Phys. B* **237** (1984) 307, doi:10.1016/0550-3213(84)90162-7.

[29] M. Drees, "Supersymmetric models with extended Higgs sector", *Int. J. Mod. Phys. A* **4** (1989) 3635, doi:10.1142/S0217751X89001448.

[30] U. Ellwanger, C. Hugonie, and A. M. Teixeira, "The next-to-minimal supersymmetric standard model", *Phys. Rept.* **496** (2010) 1, doi:10.1016/j.physrep.2010.07.001, arXiv:0910.1785.

[31] A. Falkowski, J. T. Ruderman, T. Volansky, and J. Zupan, "Hidden Higgs decaying to lepton jets", *JHEP* **05** (2010) 077, doi:10.1007/JHEP05(2010)077, arXiv:1002.2952.

[32] CMS Collaboration, "A search for pair production of new light bosons decaying into muons in proton-proton collisions at 13 TeV", *Phys. Lett. B* **796** (2019) 131, doi:10.1016/j.physletb.2019.07.013, arXiv:1812.00380.

[33] ATLAS Collaboration, "Search for long-lived neutral particles decaying into lepton jets in proton-proton collisions at $\sqrt{s} = 8$ TeV with the ATLAS detector", *JHEP* **11** (2014) 088, doi:10.1007/JHEP11(2014)088, arXiv:1409.0746.

[34] ATLAS Collaboration, "Search for displaced muonic lepton jets from light Higgs boson decay in proton-proton collisions at $\sqrt{s} = 7$ TeV with the ATLAS detector", *Phys. Lett. B* **721** (2013) 32, doi:10.1016/j.physletb.2013.02.058, arXiv:1210.0435.

[35] CMS Collaboration, "Search for light resonances decaying into pairs of muons as a signal of new physics", *JHEP* **07** (2011) 098, doi:10.1007/JHEP07(2011)098, arXiv:1106.2375.

[36] CMS Collaboration, "Search For a non-standard-model Higgs boson decaying to a pair of new light bosons in four-muon final states", *Phys. Lett. B* **726** (2013) 564, doi:10.1016/j.physletb.2013.09.009, arXiv:1210.7619.

[37] CMS Collaboration, “A search for pair production of new light bosons decaying into muons”, *Phys. Lett. B* **752** (2016) 146, doi:10.1016/j.physletb.2015.10.067, arXiv:1506.00424.

[38] CMS Collaboration, “Search for a very light NMSSM Higgs boson produced in decays of the 125 GeV scalar boson and decaying into τ leptons in pp collisions at $\sqrt{s} = 8$ TeV”, *JHEP* **01** (2016) 079, doi:10.1007/JHEP01(2016)079, arXiv:1510.06534.

[39] CMS Collaboration, “Search for light pseudoscalar boson pairs produced from decays of the 125 GeV Higgs boson in final states with two muons and two nearby tracks in pp collisions at $\sqrt{s} = 13$ TeV”, *Phys. Lett. B* **800** (2020) 135087, doi:10.1016/j.physletb.2019.135087, arXiv:1907.07235.

[40] CMS Collaboration, “Search for low-mass dilepton resonances in Higgs boson decays to four-lepton final states in proton–proton collisions at $\sqrt{s} = 13$ TeV”, *Eur. Phys. J. C* **82** (2022) 290, doi:10.1140/epjc/s10052-022-10127-0, arXiv:2111.01299.

[41] ATLAS Collaboration, “Search for new light gauge bosons in Higgs boson decays to four-lepton final states in pp collisions at $\sqrt{s} = 8$ TeV with the ATLAS detector at the LHC”, *Phys. Rev. D* **92** (2015) 092001, doi:10.1103/PhysRevD.92.092001, arXiv:1505.07645.

[42] ATLAS Collaboration, “Search for Higgs boson decays to beyond-the-Standard-Model light bosons in four-lepton events with the ATLAS detector at $\sqrt{s} = 13$ TeV”, *JHEP* **06** (2018) 166, doi:10.1007/JHEP06(2018)166, arXiv:1802.03388.

[43] ATLAS Collaboration, “A search for prompt lepton-jets in pp collisions at $\sqrt{s} = 8$ TeV with the ATLAS detector”, *JHEP* **02** (2016) 062, doi:10.1007/JHEP02(2016)062, arXiv:1511.05542.

[44] ATLAS Collaboration, “Search for the Higgs boson produced in association with a W boson and decaying to four b-quarks via two spin-zero particles in pp collisions at 13 TeV with the ATLAS detector”, *Eur. Phys. J. C* **76** (2016) 605, doi:10.1140/epjc/s10052-016-4418-9, arXiv:1606.08391.

[45] ATLAS Collaboration, “Search for the Higgs boson produced in association with a vector boson and decaying into two spin-zero particles in the $H \to aa \to 4b$ channel in pp collisions at $\sqrt{s} = 13$ TeV with the ATLAS detector”, *JHEP* **10** (2018) 031, doi:10.1007/JHEP10(2018)031, arXiv:1806.07355.

[46] ATLAS Collaboration, “Search for new phenomena in events with at least three photons collected in pp collisions at $\sqrt{s}$ = 8 TeV with the ATLAS detector”, *Eur. Phys. J. C* **76** (2016) 210, doi:10.1140/epjc/s10052-016-4034-8, arXiv:1509.05051.

[47] CMS Collaboration, “Search for an exotic decay of the Higgs boson to a pair of light pseudoscalars in the final state with two b quarks and two τ leptons in proton-proton collisions at $\sqrt{s} = 13$ TeV”, *Phys. Lett. B* **785** (2018) 462, doi:10.1016/j.physletb.2018.08.057, arXiv:1805.10191.

[48] CMS Collaboration, “Search for exotic decays of the Higgs boson to a pair of pseudoscalars in the $\mu\mu$bb and $\tau\tau$bb final states”, *Eur. Phys. J. C* **84** (2024), no. 5, 493, doi:10.1140/epjc/s10052-024-12727-4, arXiv:2402.13358.

[49] CMS Collaboration, "Search for an exotic decay of the Higgs boson to a pair of light pseudoscalars in the final state of two muons and two τ leptons in proton-proton collisions at $\sqrt{s} = 13$ TeV", *JHEP* **11** (2018) 018, doi:10.1007/JHEP11(2018)018, arXiv:1805.04865.

[50] CMS Collaboration, "Search for a light pseudoscalar Higgs boson in the boosted $\mu\mu\tau\tau$ final state in proton-proton collisions at $\sqrt{s} = 13$ TeV", *JHEP* **08** (2020) 139, doi:10.1007/JHEP08(2020)139, arXiv:2005.08694.

[51] LHCb Collaboration, "Search for Higgs-like bosons decaying into long-lived exotic particles", *Eur. Phys. J. C* **76** (2016) 664, doi:10.1140/epjc/s10052-016-4489-7, arXiv:1609.03124.

[52] CMS Collaboration, "Search for a narrow resonance lighter than 200 GeV decaying to a pair of muons in proton-proton collisions at $\sqrt{s} = 13$ TeV", *Phys. Rev. Lett.* **124** (2020) 131802, doi:10.1103/PhysRevLett.124.131802, arXiv:1912.04776.

[53] CMS Collaboration, "Search for direct production of GeV-scale resonances decaying to a pair of muons in proton-proton collisions at $\sqrt{s}$ = 13 TeV", *JHEP* **12** (2023) 070, doi:10.1007/JHEP12(2023)070, arXiv:2309.16003.

[54] CMS Collaboration, "Search for long-lived particles decaying into muon pairs in proton-proton collisions at $\sqrt{s}$ = 13 TeV collected with a dedicated high-rate data stream", *JHEP* **04** (2022) 062, doi:10.1007/JHEP04(2022)062, arXiv:2112.13769.

[55] CMS Collaboration, "Search for long-lived particles decaying to a pair of muons in proton-proton collisions at $\sqrt{s}$ = 13 TeV", *JHEP* **05** (2023) 228, doi:10.1007/JHEP05(2023)228, arXiv:2205.08582.

[56] CMS Collaboration, "CMS technical design report for the pixel detector upgrade", technical report, 9, 2012. doi:10.2172/1151650.

[57] CMS Collaboration, "Calibration and performance of the CMS pixel detector in LHC Run 2", *PoS* **LHCP2019** (2019) 010, doi:10.22323/1.350.0010, arXiv:1909.12920.

[58] CMS Collaboration, "Performance of the CMS level-1 trigger in proton-proton collisions at $\sqrt{s} = 13$ TeV", *JINST* **15** (2020) P10017, doi:10.1088/1748-0221/15/10/P10017, arXiv:2006.10165.

[59] HEPData record for this analysis, 2024. doi:10.17182/hepdata.150033.

[60] CMS Collaboration, "Performance of the CMS muon detector and muon reconstruction with proton-proton collisions at $\sqrt{s} = 13$ TeV", *JINST* **13** (2018) P06015, doi:10.1088/1748-0221/13/06/P06015, arXiv:1804.04528.

[61] CMS Collaboration, "The CMS trigger system", *JINST* **12** (2017) P01020, doi:10.1088/1748-0221/12/01/P01020, arXiv:1609.02366.

[62] CMS Collaboration, "The CMS experiment at the CERN LHC", *JINST* **3** (2008) S08004, doi:10.1088/1748-0221/3/08/S08004.

[63] J. Alwall et al., "The automated computation of tree-level and next-to-leading order differential cross sections, and their matching to parton shower simulations", *JHEP* **07** (2014) 079, doi:10.1007/JHEP07(2014)079, arXiv:1405.0301.

[64] P. Artoisenet, R. Frederix, O. Mattelaer, and R. Rietkerk, “Automatic spin-entangled decays of heavy resonances in Monte Carlo simulations”, *JHEP* **03** (2013) 015, doi:10.1007/JHEP03(2013)015, arXiv:1212.3460.

[65] T. Sjöstrand et al., “An introduction to PYTHIA 8.2”, *Comput. Phys. Commun.* **191** (2015) 159, doi:10.1016/j.cpc.2015.01.024, arXiv:1410.3012.

[66] ATLAS Collaboration, “Observation of a new particle in the search for the standard model Higgs boson with the ATLAS detector at the LHC”, *Phys. Lett. B* **716** (2012) 1, doi:10.1016/j.physletb.2012.08.020, arXiv:1207.7214.

[67] CMS Collaboration, “Observation of a new boson at a mass of 125 GeV with the CMS Experiment at the LHC”, *Phys. Lett. B* **716** (2012) 30, doi:10.1016/j.physletb.2012.08.021, arXiv:1207.7235.

[68] CMS Collaboration, “Observation of a new boson with mass near 125 GeV in pp collisions at $\sqrt{s} = 7$ and 8 TeV”, *JHEP* **06** (2013) 081, doi:10.1007/JHEP06(2013)081, arXiv:1303.4571.

[69] WMAP Collaboration, “Nine-year Wilkinson microwave anisotropy probe (WMAP) observations: Cosmological parameter results”, *Astrophys. J. Suppl.* **208** (2013) 19, doi:10.1088/0067-0049/208/2/19, arXiv:1212.5226.

[70] Planck Collaboration, “Planck 2013 results. XVI. cosmological parameters”, *Astron. Astrophys.* **571** (2014) A16, doi:10.1051/0004-6361/201321591, arXiv:1303.5076.

[71] OPAL Collaboration, “Decay mode independent searches for new scalar bosons with the OPAL detector at LEP”, *Eur. Phys. J. C* **27** (2003) 311, doi:10.1140/epjc/s2002-01115-1, arXiv:hep-ex/0206022.

[72] OPAL Collaboration, “Search for a low mass CP odd Higgs boson in e+ e- collisions with the OPAL detector at LEP-2”, *Eur. Phys. J. C* **27** (2003) 483, doi:10.1140/epjc/s2003-01139-y, arXiv:hep-ex/0209068.

[73] OPAL Collaboration, “Search for neutral Higgs boson in CP-conserving and CP-violating MSSM scenarios”, *Eur. Phys. J. C* **37** (2004) 49, doi:10.1140/epjc/s2004-01962-6, arXiv:hep-ex/0406057.

[74] DELPHI Collaboration, “Searches for neutral Higgs bosons in extended models”, *Eur. Phys. J. C* **38** (2004) 1, doi:10.1140/epjc/s2004-02011-4, arXiv:hep-ex/0410017.

[75] ALEPH Collaboration, “Search for neutral Higgs bosons decaying into four taus at LEP2”, *JHEP* **05** (2010) 049, doi:10.1007/JHEP05(2010)049, arXiv:1003.0705.

[76] ALEPH, DELPHI, L3, OPAL, LEP Working Group for Higgs Boson Searches Collaboration, “Search for neutral MSSM Higgs bosons at LEP”, *Eur. Phys. J. C* **47** (2006) 547, doi:10.1140/epjc/s2006-02569-7, arXiv:hep-ex/0602042.

[77] R. Dermisek and J. F. Gunion, “New constraints on a light CP-odd Higgs boson and related NMSSM ideal Higgs scenarios”, *Phys. Rev. D* **81** (2010) 075003, doi:10.1103/PhysRevD.81.075003, arXiv:1002.1971.

[78] NNPDF Collaboration, "Parton distributions from high-precision collider data", *Eur. Phys. J. C* **77** (2017) 663, doi:10.1140/epjc/s10052-017-5199-5, arXiv:1706.00428.

[79] CMS Collaboration, "Extraction and validation of a new set of CMS PYTHIA8 tunes from underlying-event measurements", *Eur. Phys. J. C* **80** (2020) 4, doi:10.1140/epjc/s10052-019-7499-4, arXiv:1903.12179.

[80] GEANT4 Collaboration, "GEANT4—a simulation toolkit", *Nucl. Instrum. Meth. A* **506** (2003) 250, doi:10.1016/S0168-9002(03)01368-8.

[81] CMS Collaboration, "Technical proposal for the Phase-II upgrade of the CMS Detector", technical report, 6, 2015. doi:10.17181/CERN.VU8I.D59J.

[82] CMS Collaboration, "Particle-flow reconstruction and global event description with the CMS detector", *JINST* **12** (2017) P10003, doi:10.1088/1748-0221/12/10/P10003, arXiv:1706.04965.

[83] CMS Collaboration, "Description and performance of track and primary-vertex reconstruction with the CMS tracker", *JINST* **9** (2014) P10009, doi:10.1088/1748-0221/9/10/P10009, arXiv:1405.6569.

[84] J. Gaiser et al., "Charmonium spectroscopy from inclusive psi-prime and J/psi radiative decays", *Phys. Rev. D* **34** (1986) 711, doi:10.1103/PhysRevD.34.711.

[85] S. Baker and R. D. Cousins, "Clarification of the use of chi-square and likelihood functions in fits to histograms", *Nucl. Instrum. Meth.* **221** (1984) 437, doi:10.1016/0167-5087(84)90016-4.

[86] K. S. Cranmer, "Kernel estimation in high-energy physics", *Comput. Phys. Commun.* **136** (2001) 198, doi:10.1016/S0010-4655(00)00243-5, arXiv:hep-ex/0011057.

[87] CMS Collaboration, "CMS luminosity measurement for the 2017 data-taking period at $\sqrt{s}$ = 13 TeV", CMS Physics Analysis Summary CMS-PAS-LUM-17-004, 2018.

[88] CMS Collaboration, "CMS luminosity measurement for the 2018 data-taking period at $\sqrt{s}$ = 13 TeV", CMS Physics Analysis Summary CMS-PAS-LUM-18-002, 2019.

[89] CMS Collaboration, "Search for long-lived heavy neutral leptons with displaced vertices in proton-proton collisions at $\sqrt{\text{s}}$ =13 TeV", *JHEP* **07** (2022) 081, doi:10.1007/JHEP07(2022)081, arXiv:2201.05578.

[90] CMS Collaboration, "Performance of the CMS muon trigger system in proton-proton collisions at $\sqrt{s} = 13$ TeV", *JINST* **16** (2021) P07001, doi:10.1088/1748-0221/16/07/P07001, arXiv:2102.04790.

[91] A. L. Read, "Presentation of search results: The CL_s technique", *J. Phys. G* **28** (2002) 2693, doi:10.1088/0954-3899/28/10/313.

[92] T. Junk, "Confidence level computation for combining searches with small statistics", *Nucl. Instrum. Meth. A* **434** (1999) 435, doi:10.1016/S0168-9002(99)00498-2, arXiv:hep-ex/9902006.

[93] CMS Collaboration, "Precise determination of the mass of the Higgs boson and tests of compatibility of its couplings with the standard model predictions using proton collisions at 7 and 8 TeV", *Eur. Phys. J. C* **75** (2015) 212, doi:10.1140/epjc/s10052-015-3351-7, arXiv:1412.8662.

[94] CMS Collaboration, "The CMS statistical analysis and combination tool: COMBINE", 2024. arXiv:2404.06614. Submitted to *Comput. Softw. Big Sci.*

[95] M. Cepeda et al., "Report from working group 2: Higgs physics at the HL-LHC and HE-LHC", *CERN Yellow Rep. Monogr.* **7** (2019) 221, doi:10.23731/CYRM-2019-007.221, arXiv:1902.00134.

[96] ATLAS Collaboration, "Search for Higgs bosons decaying to aa in the $\mu\mu\tau\tau$ final state in pp collisions at $\sqrt{s} = 8$ TeV with the ATLAS experiment", *Phys. Rev. D* **92** (2015) 052002, doi:10.1103/PhysRevD.92.052002, arXiv:1505.01609.

[97] CMS Collaboration, "Search for light bosons in decays of the 125 GeV Higgs boson in proton-proton collisions at $\sqrt{s} = 8$ TeV", *JHEP* **10** (2017) 076, doi:10.1007/JHEP10(2017)076, arXiv:1701.02032.

[98] B. Batell, M. Pospelov, and A. Ritz, "Probing a secluded U(1) at B-factories", *Phys. Rev. D* **79** (2009) 115008, doi:10.1103/PhysRevD.79.115008, arXiv:0903.0363.

A The CMS Collaboration

Yerevan Physics Institute, Yerevan, Armenia
A. Hayrapetyan, A. Tumasyan[1]

Institut für Hochenergiephysik, Vienna, Austria
W. Adam, J.W. Andrejkovic, T. Bergauer, S. Chatterjee, K. Damanakis, M. Dragicevic, P.S. Hussain, M. Jeitler[2], N. Krammer, A. Li, D. Liko, I. Mikulec, J. Schieck[2], R. Schöfbeck, D. Schwarz, M. Sonawane, S. Templ, W. Waltenberger, C.-E. Wulz[2]

Universiteit Antwerpen, Antwerpen, Belgium
M.R. Darwish[3], T. Janssen, T. Van Laer, P. Van Mechelen

Vrije Universiteit Brussel, Brussel, Belgium
N. Breugelmans, J. D'Hondt, S. Dansana, A. De Moor, M. Delcourt, F. Heyen, S. Lowette, I. Makarenko, D. Müller, S. Tavernier, M. Tytgat[4], G.P. Van Onsem, S. Van Putte, D. Vannerom

Université Libre de Bruxelles, Bruxelles, Belgium
B. Bilin, B. Clerbaux, A.K. Das, G. De Lentdecker, H. Evard, L. Favart, P. Gianneios, J. Jaramillo, A. Khalilzadeh, F.A. Khan, K. Lee, M. Mahdavikhorrami, A. Malara, S. Paredes, M.A. Shahzad, L. Thomas, M. Vanden Bemden, C. Vander Velde, P. Vanlaer

Ghent University, Ghent, Belgium
M. De Coen, D. Dobur, G. Gokbulut, Y. Hong, J. Knolle, L. Lambrecht, D. Marckx, K. Mota Amarilo, A. Samalan, K. Skovpen, N. Van Den Bossche, J. van der Linden, L. Wezenbeek

Université Catholique de Louvain, Louvain-la-Neuve, Belgium
A. Benecke, A. Bethani, G. Bruno, C. Caputo, J. De Favereau De Jeneret, C. Delaere, I.S. Donertas, A. Giammanco, A.O. Guzel, Sa. Jain, V. Lemaitre, J. Lidrych, P. Mastrapasqua, T.T. Tran, S. Wertz

Centro Brasileiro de Pesquisas Fisicas, Rio de Janeiro, Brazil
G.A. Alves, M. Alves Gallo Pereira, E. Coelho, G. Correia Silva, C. Hensel, T. Menezes De Oliveira, C. Mora Herrera[5], A. Moraes, P. Rebello Teles, M. Soeiro, A. Vilela Pereira[5]

Universidade do Estado do Rio de Janeiro, Rio de Janeiro, Brazil
W.L. Aldá Júnior, M. Barroso Ferreira Filho, H. Brandao Malbouisson, W. Carvalho, J. Chinellato[6], E.M. Da Costa, G.G. Da Silveira[7], D. De Jesus Damiao, S. Fonseca De Souza, R. Gomes De Souza, M. Macedo, J. Martins[8], L. Mundim, H. Nogima, J.P. Pinheiro, A. Santoro, A. Sznajder, M. Thiel

Universidade Estadual Paulista, Universidade Federal do ABC, São Paulo, Brazil
C.A. Bernardes[7], L. Calligaris, T.R. Fernandez Perez Tomei, E.M. Gregores, B. Lopes Da Costa, I. Maietto Silverio, P.G. Mercadante, S.F. Novaes, B. Orzari, Sandra S. Padula

Institute for Nuclear Research and Nuclear Energy, Bulgarian Academy of Sciences, Sofia, Bulgaria
A. Aleksandrov, G. Antchev, R. Hadjiiska, P. Iaydjiev, M. Misheva, M. Shopova, G. Sultanov

University of Sofia, Sofia, Bulgaria
A. Dimitrov, L. Litov, B. Pavlov, P. Petkov, A. Petrov, E. Shumka

Instituto De Alta Investigación, Universidad de Tarapacá, Casilla 7 D, Arica, Chile
S. Keshri, S. Thakur

Beihang University, Beijing, China
T. Cheng, T. Javaid, L. Yuan

Department of Physics, Tsinghua University, Beijing, China
Z. Hu, Z. Liang, J. Liu, K. Yi[9,10]

Institute of High Energy Physics, Beijing, China
G.M. Chen[11], H.S. Chen[11], M. Chen[11], F. Iemmi, C.H. Jiang, A. Kapoor[12], H. Liao, Z.-A. Liu[13], R. Sharma[14], J.N. Song[13], J. Tao, C. Wang[11], J. Wang, Z. Wang[11], H. Zhang, J. Zhao

State Key Laboratory of Nuclear Physics and Technology, Peking University, Beijing, China
A. Agapitos, Y. Ban, S. Deng, B. Guo, C. Jiang, A. Levin, C. Li, Q. Li, Y. Mao, S. Qian, S.J. Qian, X. Qin, X. Sun, D. Wang, H. Yang, L. Zhang, Y. Zhao, C. Zhou

Guangdong Provincial Key Laboratory of Nuclear Science and Guangdong-Hong Kong Joint Laboratory of Quantum Matter, South China Normal University, Guangzhou, China
S. Yang

Sun Yat-Sen University, Guangzhou, China
Z. You

University of Science and Technology of China, Hefei, China
K. Jaffel, N. Lu

Nanjing Normal University, Nanjing, China
G. Bauer[15], B. Li, J. Zhang

Institute of Modern Physics and Key Laboratory of Nuclear Physics and Ion-beam Application (MOE) - Fudan University, Shanghai, China
X. Gao[16]

Zhejiang University, Hangzhou, Zhejiang, China
Z. Lin, C. Lu, M. Xiao

Universidad de Los Andes, Bogota, Colombia
C. Avila, D.A. Barbosa Trujillo, A. Cabrera, C. Florez, J. Fraga, J.A. Reyes Vega

Universidad de Antioquia, Medellin, Colombia
F. Ramirez, C. Rendón, M. Rodriguez, A.A. Ruales Barbosa, J.D. Ruiz Alvarez

University of Split, Faculty of Electrical Engineering, Mechanical Engineering and Naval Architecture, Split, Croatia
D. Giljanovic, N. Godinovic, D. Lelas, A. Sculac

University of Split, Faculty of Science, Split, Croatia
M. Kovac, A. Petkovic, T. Sculac

Institute Rudjer Boskovic, Zagreb, Croatia
P. Bargassa, V. Brigljevic, B.K. Chitroda, D. Ferencek, K. Jakovcic, S. Mishra, A. Starodumov[17], T. Susa

University of Cyprus, Nicosia, Cyprus
A. Attikis, K. Christoforou, A. Hadjiagapiou, C. Leonidou, J. Mousa, C. Nicolaou, L. Paizanos, F. Ptochos, P.A. Razis, H. Rykaczewski, H. Saka, A. Stepennov

Charles University, Prague, Czech Republic
M. Finger, M. Finger Jr., A. Kveton

Universidad San Francisco de Quito, Quito, Ecuador
E. Carrera Jarrin

Academy of Scientific Research and Technology of the Arab Republic of Egypt, Egyptian Network of High Energy Physics, Cairo, Egypt
Y. Assran[18,19], B. El-mahdy, S. Elgammal[19]

Center for High Energy Physics (CHEP-FU), Fayoum University, El-Fayoum, Egypt
A. Lotfy, Y. Mohammed

National Institute of Chemical Physics and Biophysics, Tallinn, Estonia
K. Ehataht, M. Kadastik, T. Lange, S. Nandan, C. Nielsen, J. Pata, M. Raidal, L. Tani, C. Veelken

Department of Physics, University of Helsinki, Helsinki, Finland
H. Kirschenmann, K. Osterberg, M. Voutilainen

Helsinki Institute of Physics, Helsinki, Finland
S. Bharthuar, N. Bin Norjoharuddeen, E. Brücken, F. Garcia, P. Inkaew, K.T.S. Kallonen, T. Lampén, K. Lassila-Perini, S. Lehti, T. Lindén, L. Martikainen, M. Myllymäki, M.m. Rantanen, H. Siikonen, J. Tuominiemi

Lappeenranta-Lahti University of Technology, Lappeenranta, Finland
P. Luukka, H. Petrow

IRFU, CEA, Université Paris-Saclay, Gif-sur-Yvette, France
M. Besancon, F. Couderc, M. Dejardin, D. Denegri, J.L. Faure, F. Ferri, S. Ganjour, P. Gras, G. Hamel de Monchenault, M. Kumar, V. Lohezic, J. Malcles, F. Orlandi, L. Portales, A. Rosowsky, M.Ö. Sahin, A. Savoy-Navarro[20], P. Simkina, M. Titov, M. Tornago

Laboratoire Leprince-Ringuet, CNRS/IN2P3, Ecole Polytechnique, Institut Polytechnique de Paris, Palaiseau, France
F. Beaudette, G. Boldrini, P. Busson, A. Cappati, C. Charlot, M. Chiusi, F. Damas, O. Davignon, A. De Wit, I.T. Ehle, B.A. Fontana Santos Alves, S. Ghosh, A. Gilbert, R. Granier de Cassagnac, A. Hakimi, B. Harikrishnan, L. Kalipoliti, G. Liu, M. Nguyen, C. Ochando, R. Salerno, J.B. Sauvan, Y. Sirois, L. Urda Gómez, E. Vernazza, A. Zabi, A. Zghiche

Université de Strasbourg, CNRS, IPHC UMR 7178, Strasbourg, France
J.-L. Agram[21], J. Andrea, D. Apparu, D. Bloch, J.-M. Brom, E.C. Chabert, C. Collard, S. Falke, U. Goerlach, R. Haeberle, A.-C. Le Bihan, M. Meena, O. Poncet, G. Saha, M.A. Sessini, P. Van Hove, P. Vaucelle

Centre de Calcul de l'Institut National de Physique Nucleaire et de Physique des Particules, CNRS/IN2P3, Villeurbanne, France
A. Di Florio

Institut de Physique des 2 Infinis de Lyon (IP2I), Villeurbanne, France

D. Amram, S. Beauceron, B. Blancon, G. Boudoul, N. Chanon, D. Contardo, P. Depasse, C. Dozen[22], H. El Mamouni, J. Fay, S. Gascon, M. Gouzevitch, C. Greenberg, G. Grenier, B. Ille, E. Jourd'huy, I.B. Laktineh, M. Lethuillier, L. Mirabito, S. Perries, A. Purohit, M. Vander Donckt, P. Verdier, J. Xiao

Georgian Technical University, Tbilisi, Georgia
I. Bagaturia[23], I. Lomidze, Z. Tsamalaidze[17]

RWTH Aachen University, I. Physikalisches Institut, Aachen, Germany
V. Botta, S. Consuegra Rodríguez, L. Feld, K. Klein, M. Lipinski, D. Meuser, A. Pauls, D. Pérez Adán, N. Röwert, M. Teroerde

RWTH Aachen University, III. Physikalisches Institut A, Aachen, Germany
S. Diekmann, A. Dodonova, N. Eich, D. Eliseev, F. Engelke, J. Erdmann, M. Erdmann, P. Fackeldey, B. Fischer, T. Hebbeker, K. Hoepfner, F. Ivone, A. Jung, M.y. Lee, F. Mausolf, M. Merschmeyer, A. Meyer, S. Mukherjee, D. Noll, F. Nowotny, A. Pozdnyakov, Y. Rath, W. Redjeb, F. Rehm, H. Reithler, V. Sarkisovi, A. Schmidt, A. Sharma, J.L. Spah, A. Stein, F. Torres Da Silva De Araujo[24], S. Wiedenbeck, S. Zaleski

RWTH Aachen University, III. Physikalisches Institut B, Aachen, Germany
C. Dziwok, G. Flügge, T. Kress, A. Nowack, O. Pooth, A. Stahl, T. Ziemons, A. Zotz

Deutsches Elektronen-Synchrotron, Hamburg, Germany
H. Aarup Petersen, M. Aldaya Martin, J. Alimena, S. Amoroso, Y. An, J. Bach, S. Baxter, M. Bayatmakou, H. Becerril Gonzalez, O. Behnke, A. Belvedere, S. Bhattacharya, F. Blekman[25], K. Borras[26], A. Campbell, A. Cardini, C. Cheng, F. Colombina, M. De Silva, G. Eckerlin, D. Eckstein, L.I. Estevez Banos, O. Filatov, E. Gallo[25], A. Geiser, V. Guglielmi, M. Guthoff, A. Hinzmann, L. Jeppe, B. Kaech, M. Kasemann, C. Kleinwort, R. Kogler, M. Komm, D. Krücker, W. Lange, D. Leyva Pernia, K. Lipka[27], W. Lohmann[28], F. Lorkowski, R. Mankel, I.-A. Melzer-Pellmann, M. Mendizabal Morentin, A.B. Meyer, G. Milella, K. Moral Figueroa, A. Mussgiller, L.P. Nair, J. Niedziela, A. Nürnberg, Y. Otarid, J. Park, E. Ranken, A. Raspereza, D. Rastorguev, J. Rübenach, L. Rygaard, A. Saggio, M. Scham[29,26], S. Schnake[26], P. Schütze, C. Schwanenberger[25], D. Selivanova, K. Sharko, M. Shchedrolosiev, D. Stafford, F. Vazzoler, A. Ventura Barroso, R. Walsh, D. Wang, Q. Wang, Y. Wen, K. Wichmann, L. Wiens[26], C. Wissing, Y. Yang, A. Zimermmane Castro Santos

University of Hamburg, Hamburg, Germany
A. Albrecht, S. Albrecht, M. Antonello, S. Bein, L. Benato, S. Bollweg, M. Bonanomi, P. Connor, K. El Morabit, Y. Fischer, E. Garutti, A. Grohsjean, J. Haller, H.R. Jabusch, G. Kasieczka, P. Keicher, R. Klanner, W. Korcari, T. Kramer, C.c. Kuo, V. Kutzner, F. Labe, J. Lange, A. Lobanov, C. Matthies, L. Moureaux, M. Mrowietz, A. Nigamova, Y. Nissan, A. Paasch, K.J. Pena Rodriguez, T. Quadfasel, B. Raciti, M. Rieger, D. Savoiu, J. Schindler, P. Schleper, M. Schröder, J. Schwandt, M. Sommerhalder, H. Stadie, G. Steinbrück, A. Tews, M. Wolf

Karlsruher Institut fuer Technologie, Karlsruhe, Germany
S. Brommer, M. Burkart, E. Butz, T. Chwalek, A. Dierlamm, A. Droll, N. Faltermann, M. Giffels, A. Gottmann, F. Hartmann[30], R. Hofsaess, M. Horzela,

U. Husemann, J. Kieseler, M. Klute, R. Koppenhöfer, J.M. Lawhorn, M. Link, A. Lintuluoto, B. Maier, S. Maier, S. Mitra, M. Mormile, Th. Müller, M. Neukum, M. Oh, E. Pfeffer, M. Presilla, G. Quast, K. Rabbertz, B. Regnery, N. Shadskiy, I. Shvetsov, H.J. Simonis, L. Sowa, L. Stockmeier, K. Tauqeer, M. Toms, N. Trevisani, R.F. Von Cube, M. Wassmer, S. Wieland, F. Wittig, R. Wolf, X. Zuo

Institute of Nuclear and Particle Physics (INPP), NCSR Demokritos, Aghia Paraskevi, Greece
G. Anagnostou, G. Daskalakis, A. Kyriakis, A. Papadopoulos[30], A. Stakia

National and Kapodistrian University of Athens, Athens, Greece
P. Kontaxakis, G. Melachroinos, Z. Painesis, I. Papavergou, I. Paraskevas, N. Saoulidou, K. Theofilatos, E. Tziaferi, K. Vellidis, I. Zisopoulos

National Technical University of Athens, Athens, Greece
G. Bakas, T. Chatzistavrou, G. Karapostoli, K. Kousouris, I. Papakrivopoulos, E. Siamarkou, G. Tsipolitis, A. Zacharopoulou

University of Ioánnina, Ioánnina, Greece
K. Adamidis, I. Bestintzanos, I. Evangelou, C. Foudas, C. Kamtsikis, P. Katsoulis, P. Kokkas, P.G. Kosmoglou Kioseoglou, N. Manthos, I. Papadopoulos, J. Strologas

HUN-REN Wigner Research Centre for Physics, Budapest, Hungary
C. Hajdu, D. Horvath[31,32], K. Márton, A.J. Rádl[33], F. Sikler, V. Veszpremi

MTA-ELTE Lendület CMS Particle and Nuclear Physics Group, Eötvös Loránd University, Budapest, Hungary
M. Csanád, K. Farkas, A. Fehérkuti[34], M.M.A. Gadallah[35], Á. Kadlecsik, P. Major, G. Pásztor, G.I. Veres

Faculty of Informatics, University of Debrecen, Debrecen, Hungary
B. Ujvari, G. Zilizi

Institute of Nuclear Research ATOMKI, Debrecen, Hungary
G. Bencze, S. Czellar, J. Molnar, Z. Szillasi

Karoly Robert Campus, MATE Institute of Technology, Gyongyos, Hungary
F. Nemes[34], T. Novak

Panjab University, Chandigarh, India
J. Babbar, S. Bansal, S.B. Beri, V. Bhatnagar, G. Chaudhary, S. Chauhan, N. Dhingra[36], A. Kaur, A. Kaur, H. Kaur, M. Kaur, S. Kumar, K. Sandeep, T. Sheokand, J.B. Singh, A. Singla

University of Delhi, Delhi, India
A. Ahmed, A. Bhardwaj, A. Chhetri, B.C. Choudhary, A. Kumar, A. Kumar, M. Naimuddin, K. Ranjan, M.K. Saini, S. Saumya

Saha Institute of Nuclear Physics, HBNI, Kolkata, India
S. Baradia, S. Barman[37], S. Bhattacharya, S. Das Gupta, S. Dutta, S. Dutta, S. Sarkar

Indian Institute of Technology Madras, Madras, India
M.M. Ameen, P.K. Behera, S.C. Behera, S. Chatterjee, G. Dash, P. Jana, P. Kalbhor, S. Kamble, J.R. Komaragiri[38], D. Kumar[38], P.R. Pujahari, N.R. Saha, A. Sharma, A.K. Sikdar, R.K. Singh, P. Verma, S. Verma, A. Vijay

Tata Institute of Fundamental Research-A, Mumbai, India
S. Dugad, G.B. Mohanty, B. Parida, M. Shelake, P. Suryadevara

Tata Institute of Fundamental Research-B, Mumbai, India
A. Bala, S. Banerjee, R.M. Chatterjee, M. Guchait, Sh. Jain, A. Jaiswal, S. Kumar, G. Majumder, K. Mazumdar, S. Parolia, A. Thachayath

National Institute of Science Education and Research, An OCC of Homi Bhabha National Institute, Bhubaneswar, Odisha, India
S. Bahinipati[39], C. Kar, D. Maity[40], P. Mal, T. Mishra, V.K. Muraleedharan Nair Bindhu[40], K. Naskar[40], A. Nayak[40], S. Nayak, K. Pal, P. Sadangi, S.K. Swain, S. Varghese[40], D. Vats[40]

Indian Institute of Science Education and Research (IISER), Pune, India
S. Acharya[41], A. Alpana, S. Dube, B. Gomber[41], P. Hazarika, B. Kansal, A. Laha, B. Sahu[41], S. Sharma, K.Y. Vaish

Isfahan University of Technology, Isfahan, Iran
H. Bakhshiansohi[42], A. Jafari[43], M. Zeinali[44]

Institute for Research in Fundamental Sciences (IPM), Tehran, Iran
S. Bashiri, S. Chenarani[45], S.M. Etesami, Y. Hosseini, M. Khakzad, E. Khazaie[46], M. Mohammadi Najafabadi, S. Tizchang[47]

University College Dublin, Dublin, Ireland
M. Felcini, M. Grunewald

INFN Sezione di Bari[a], Università di Bari[b], Politecnico di Bari[c], Bari, Italy
M. Abbrescia[a,b], A. Colaleo[a,b], D. Creanza[a,c], B. D'Anzi[a,b], N. De Filippis[a,c], M. De Palma[a,b], W. Elmetenawee[a,b,48], L. Fiore[a], G. Iaselli[a,c], L. Longo[a], M. Louka[a,b], G. Maggi[a,c], M. Maggi[a], I. Margjeka[a], V. Mastrapasqua[a,b], S. My[a,b], S. Nuzzo[a,b], A. Pellecchia[a,b], A. Pompili[a,b], G. Pugliese[a,c], R. Radogna[a,b], D. Ramos[a], A. Ranieri[a], L. Silvestris[a], F.M. Simone[a,c], Ü. Sözbilir[a], A. Stamerra[a,b], D. Troiano[a,b], R. Venditti[a,b], P. Verwilligen[a], A. Zaza[a,b]

INFN Sezione di Bologna[a], Università di Bologna[b], Bologna, Italy
G. Abbiendi[a], C. Battilana[a,b], D. Bonacorsi[a,b], P. Capiluppi[a,b], A. Castro[†a,b], F.R. Cavallo[a], M. Cuffiani[a,b], G.M. Dallavalle[a], T. Diotalevi[a,b], F. Fabbri[a], A. Fanfani[a,b], D. Fasanella[a], P. Giacomelli[a], L. Giommi[a,b], C. Grandi[a], L. Guiducci[a,b], S. Lo Meo[a,49], M. Lorusso[a,b], L. Lunerti[a], S. Marcellini[a], G. Masetti[a], F.L. Navarria[a,b], G. Paggi[a,b], A. Perrotta[a], F. Primavera[a,b], A.M. Rossi[a,b], S. Rossi Tisbeni[a,b], T. Rovelli[a,b], G.P. Siroli[a,b]

INFN Sezione di Catania[a], Università di Catania[b], Catania, Italy
S. Costa[a,b,50], A. Di Mattia[a], A. Lapertosa[a], R. Potenza[a,b], A. Tricomi[a,b,50], C. Tuve[a,b]

INFN Sezione di Firenze[a], Università di Firenze[b], Firenze, Italy
P. Assiouras[a], G. Barbagli[a], G. Bardelli[a,b], B. Camaiani[a,b], A. Cassese[a], R. Ceccarelli[a], V. Ciulli[a,b], C. Civinini[a], R. D'Alessandro[a,b], E. Focardi[a,b], T. Kello[a], G. Latino[a,b], P. Lenzi[a,b], M. Lizzo[a], M. Meschini[a], S. Paoletti[a], A. Papanastassiou[a,b], G. Sguazzoni[a], L. Viliani[a]

INFN Laboratori Nazionali di Frascati, Frascati, Italy
L. Benussi, S. Bianco, S. Meola[51], D. Piccolo

INFN Sezione di Genova[a], Università di Genova[b], Genova, Italy
P. Chatagnon[a], F. Ferro[a], E. Robutti[a], S. Tosi[a,b]

INFN Sezione di Milano-Bicocca[a], Università di Milano-Bicocca[b], Milano, Italy
A. Benaglia[a], F. Brivio[a], F. Cetorelli[a,b], F. De Guio[a,b], M.E. Dinardo[a,b], P. Dini[a], S. Gennai[a], R. Gerosa[a,b], A. Ghezzi[a,b], P. Govoni[a,b], L. Guzzi[a], M.T. Lucchini[a,b], M. Malberti[a], S. Malvezzi[a], A. Massironi[a], D. Menasce[a], L. Moroni[a], M. Paganoni[a,b], S. Palluotto[a,b], D. Pedrini[a], A. Perego[a,b], B.S. Pinolini[a], G. Pizzati[a,b], S. Ragazzi[a,b], T. Tabarelli de Fatis[a,b]

INFN Sezione di Napoli[a], Università di Napoli 'Federico II'[b], Napoli, Italy; Università della Basilicata[c], Potenza, Italy; Scuola Superiore Meridionale (SSM)[d], Napoli, Italy
S. Buontempo[a], A. Cagnotta[a,b], F. Carnevali[a,b], N. Cavallo[a,c], F. Fabozzi[a,c], A.O.M. Iorio[a,b], L. Lista[a,b,52], P. Paolucci[a,30]

INFN Sezione di Padova[a], Università di Padova[b], Padova, Italy; Università di Trento[c], Trento, Italy
R. Ardino[a], P. Azzi[a], N. Bacchetta[a,53], D. Bisello[a,b], P. Bortignon[a], G. Bortolato[a,b], A. Bragagnolo[a,b], A.C.M. Bulla[a], R. Carlin[a,b], T. Dorigo[a], F. Gasparini[a,b], U. Gasparini[a,b], E. Lusiani[a], M. Margoni[a,b], A.T. Meneguzzo[a,b], M. Migliorini[a,b], F. Montecassiano[a], J. Pazzini[a,b], P. Ronchese[a,b], R. Rossin[a,b], F. Simonetto[a,b], M. Tosi[a,b], A. Triossi[a,b], S. Ventura[a], M. Zanetti[a,b], P. Zotto[a,b], A. Zucchetta[a,b], G. Zumerle[a,b]

INFN Sezione di Pavia[a], Università di Pavia[b], Pavia, Italy
C. Aimè[a], A. Braghieri[a], S. Calzaferri[a], D. Fiorina[a], P. Montagna[a,b], V. Re[a], C. Riccardi[a,b], P. Salvini[a], I. Vai[a,b], P. Vitulo[a,b]

INFN Sezione di Perugia[a], Università di Perugia[b], Perugia, Italy
S. Ajmal[a,b], M.E. Ascioti[a,b], G.M. Bilei[a], C. Carrivale[a,b], D. Ciangottini[a,b], L. Fanò[a,b], M. Magherini[a,b], V. Mariani[a,b], M. Menichelli[a], F. Moscatelli[a,54], A. Rossi[a,b], A. Santocchia[a,b], D. Spiga[a], T. Tedeschi[a,b]

INFN Sezione di Pisa[a], Università di Pisa[b], Scuola Normale Superiore di Pisa[c], Pisa, Italy; Università di Siena[d], Siena, Italy
C.A. Alexe[a,c], P. Asenov[a,b], P. Azzurri[a], G. Bagliesi[a], R. Bhattacharya[a], L. Bianchini[a,b], T. Boccali[a], E. Bossini[a], D. Bruschini[a,c], R. Castaldi[a], M.A. Ciocci[a,b], M. Cipriani[a,b], V. D'Amante[a,d], R. Dell'Orso[a], S. Donato[a], A. Giassi[a], F. Ligabue[a,c], A.C. Marini[a], D. Matos Figueiredo[a], A. Messineo[a,b], M. Musich[a,b], F. Palla[a], A. Rizzi[a,b], G. Rolandi[a,c], S. Roy Chowdhury[a], T. Sarkar[a], A. Scribano[a], P. Spagnolo[a], R. Tenchini[a], G. Tonelli[a,b], N. Turini[a,d], F. Vaselli[a,c], A. Venturi[a], P.G. Verdini[a]

INFN Sezione di Roma[a], Sapienza Università di Roma[b], Roma, Italy
C. Baldenegro Barrera[a,b], P. Barria[a], C. Basile[a,b], M. Campana[a,b], F. Cavallari[a], L. Cunqueiro Mendez[a,b], D. Del Re[a,b], E. Di Marco[a,b], M. Diemoz[a], F. Errico[a,b], E. Longo[a,b], J. Mijuskovic[a,b], G. Organtini[a,b], F. Pandolfi[a], R. Paramatti[a,b], C. Quaranta[a,b], S. Rahatlou[a,b], C. Rovelli[a], F. Santanastasio[a,b], L. Soffi[a]

INFN Sezione di Torino[a], Università di Torino[b], Torino, Italy; Università del Piemonte Orientale[c], Novara, Italy
N. Amapane[a,b], R. Arcidiacono[a,c], S. Argiro[a,b], M. Arneodo[a,c], N. Bartosik[a], R. Bellan[a,b], A. Bellora[a,b], C. Biino[a], C. Borca[a,b], N. Cartiglia[a], M. Costa[a,b],

R. Covarelli[a,b], N. Demaria[a], L. Finco[a], M. Grippo[a,b], B. Kiani[a,b], F. Legger[a], F. Luongo[a,b], C. Mariotti[a], L. Markovic[a,b], S. Maselli[a], A. Mecca[a,b], L. Menzio[a,b], P. Meridiani[a], E. Migliore[a,b], M. Monteno[a], R. Mulargia[a], M.M. Obertino[a,b], G. Ortona[a], L. Pacher[a,b], N. Pastrone[a], M. Pelliccioni[a], M. Ruspa[a,c], F. Siviero[a,b], V. Sola[a,b], A. Solano[a,b], A. Staiano[a], C. Tarricone[a,b], D. Trocino[a], G. Umoret[a,b], R. White[a,b]

INFN Sezione di Trieste[a], Università di Trieste[b], Trieste, Italy
S. Belforte[a], V. Candelise[a,b], M. Casarsa[a], F. Cossutti[a], K. De Leo[a], G. Della Ricca[a,b]

Kyungpook National University, Daegu, Korea
S. Dogra, J. Hong, C. Huh, B. Kim, J. Kim, D. Lee, H. Lee, S.W. Lee, C.S. Moon, Y.D. Oh, M.S. Ryu, S. Sekmen, B. Tae, Y.C. Yang

Department of Mathematics and Physics - GWNU, Gangneung, Korea
M.S. Kim

Chonnam National University, Institute for Universe and Elementary Particles, Kwangju, Korea
G. Bak, P. Gwak, H. Kim, D.H. Moon

Hanyang University, Seoul, Korea
E. Asilar, J. Choi, D. Kim, T.J. Kim, J.A. Merlin, Y. Ryou

Korea University, Seoul, Korea
S. Choi, S. Han, B. Hong, K. Lee, K.S. Lee, S. Lee, J. Yoo

Kyung Hee University, Department of Physics, Seoul, Korea
J. Goh, S. Yang

Sejong University, Seoul, Korea
H. S. Kim, Y. Kim, S. Lee

Seoul National University, Seoul, Korea
J. Almond, J.H. Bhyun, J. Choi, J. Choi, W. Jun, J. Kim, S. Ko, H. Kwon, H. Lee, J. Lee, J. Lee, B.H. Oh, S.B. Oh, H. Seo, U.K. Yang, I. Yoon

University of Seoul, Seoul, Korea
W. Jang, D.Y. Kang, Y. Kang, S. Kim, B. Ko, J.S.H. Lee, Y. Lee, I.C. Park, Y. Roh, I.J. Watson

Yonsei University, Department of Physics, Seoul, Korea
S. Ha, H.D. Yoo

Sungkyunkwan University, Suwon, Korea
M. Choi, M.R. Kim, H. Lee, Y. Lee, I. Yu

College of Engineering and Technology, American University of the Middle East (AUM), Dasman, Kuwait
T. Beyrouthy, Y. Gharbia

Kuwait University - College of Science - Department of Physics, Safat, Kuwait
F. Alazemi

Riga Technical University, Riga, Latvia
K. Dreimanis, A. Gaile, G. Pikurs, A. Potrebko, M. Seidel, D. Sidiropoulos Kontos

University of Latvia (LU), Riga, Latvia
N.R. Strautnieks

Vilnius University, Vilnius, Lithuania
M. Ambrozas, A. Juodagalvis, A. Rinkevicius, G. Tamulaitis

National Centre for Particle Physics, Universiti Malaya, Kuala Lumpur, Malaysia
I. Yusuff[55], Z. Zolkapli

Universidad de Sonora (UNISON), Hermosillo, Mexico
J.F. Benitez, A. Castaneda Hernandez, H.A. Encinas Acosta, L.G. Gallegos Maríñez, M. León Coello, J.A. Murillo Quijada, A. Sehrawat, L. Valencia Palomo

Centro de Investigacion y de Estudios Avanzados del IPN, Mexico City, Mexico
G. Ayala, H. Castilla-Valdez, H. Crotte Ledesma, E. De La Cruz-Burelo, I. Heredia-De La Cruz[56], R. Lopez-Fernandez, J. Mejia Guisao, C.A. Mondragon Herrera, A. Sánchez Hernández

Universidad Iberoamericana, Mexico City, Mexico
C. Oropeza Barrera, D.L. Ramirez Guadarrama, M. Ramírez García

Benemerita Universidad Autonoma de Puebla, Puebla, Mexico
I. Bautista, I. Pedraza, H.A. Salazar Ibarguen, C. Uribe Estrada

University of Montenegro, Podgorica, Montenegro
I. Bubanja, N. Raicevic

University of Canterbury, Christchurch, New Zealand
P.H. Butler

National Centre for Physics, Quaid-I-Azam University, Islamabad, Pakistan
A. Ahmad, M.I. Asghar, A. Awais, M.I.M. Awan, H.R. Hoorani, W.A. Khan

AGH University of Krakow, Faculty of Computer Science, Electronics and Telecommunications, Krakow, Poland
V. Avati, L. Grzanka, M. Malawski

National Centre for Nuclear Research, Swierk, Poland
H. Bialkowska, M. Bluj, M. Górski, M. Kazana, M. Szleper, P. Zalewski

Institute of Experimental Physics, Faculty of Physics, University of Warsaw, Warsaw, Poland
K. Bunkowski, K. Doroba, A. Kalinowski, M. Konecki, J. Krolikowski, A. Muhammad

Warsaw University of Technology, Warsaw, Poland
K. Pozniak, W. Zabolotny

Laboratório de Instrumentação e Física Experimental de Partículas, Lisboa, Portugal
M. Araujo, D. Bastos, C. Beirão Da Cruz E Silva, A. Boletti, M. Bozzo, T. Camporesi, G. Da Molin, M. Gallinaro, J. Hollar, N. Leonardo, G.B. Marozzo, T. Niknejad, A. Petrilli, M. Pisano, J. Seixas, J. Varela, J.W. Wulff

Faculty of Physics, University of Belgrade, Belgrade, Serbia
P. Adzic, P. Milenovic

VINCA Institute of Nuclear Sciences, University of Belgrade, Belgrade, Serbia
M. Dordevic, J. Milosevic, V. Rekovic

Centro de Investigaciones Energéticas Medioambientales y Tecnológicas (CIEMAT), Madrid, Spain
J. Alcaraz Maestre, Cristina F. Bedoya, Oliver M. Carretero, M. Cepeda, M. Cerrada, N. Colino, B. De La Cruz, A. Delgado Peris, A. Escalante Del Valle, D. Fernández Del Val, J.P. Fernández Ramos, J. Flix, M.C. Fouz, O. Gonzalez Lopez, S. Goy Lopez, J.M. Hernandez, M.I. Josa, E. Martin Viscasillas, D. Moran, C. M. Morcillo Perez, Á. Navarro Tobar, C. Perez Dengra, A. Pérez-Calero Yzquierdo, J. Puerta Pelayo, I. Redondo, S. Sánchez Navas, J. Sastre, J. Vazquez Escobar

Universidad Autónoma de Madrid, Madrid, Spain
J.F. de Trocóniz

Universidad de Oviedo, Instituto Universitario de Ciencias y Tecnologías Espaciales de Asturias (ICTEA), Oviedo, Spain
B. Alvarez Gonzalez, J. Cuevas, J. Fernandez Menendez, S. Folgueras, I. Gonzalez Caballero, J.R. González Fernández, P. Leguina, E. Palencia Cortezon, J. Prado Pico, C. Ramón Álvarez, V. Rodríguez Bouza, A. Soto Rodríguez, A. Trapote, C. Vico Villalba, P. Vischia

Instituto de Física de Cantabria (IFCA), CSIC-Universidad de Cantabria, Santander, Spain
S. Bhowmik, S. Blanco Fernández, J.A. Brochero Cifuentes, I.J. Cabrillo, A. Calderon, J. Duarte Campderros, M. Fernandez, G. Gomez, C. Lasaosa García, R. Lopez Ruiz, C. Martinez Rivero, P. Martinez Ruiz del Arbol, F. Matorras, P. Matorras Cuevas, E. Navarrete Ramos, J. Piedra Gomez, L. Scodellaro, I. Vila, J.M. Vizan Garcia

University of Colombo, Colombo, Sri Lanka
B. Kailasapathy[57], D.D.C. Wickramarathna

University of Ruhuna, Department of Physics, Matara, Sri Lanka
W.G.D. Dharmaratna[58], K. Liyanage, N. Perera

CERN, European Organization for Nuclear Research, Geneva, Switzerland
D. Abbaneo, C. Amendola, E. Auffray, G. Auzinger, J. Baechler, D. Barney, A. Bermúdez Martínez, M. Bianco, A.A. Bin Anuar, A. Bocci, L. Borgonovi, C. Botta, E. Brondolin, C. Caillol, G. Cerminara, N. Chernyavskaya, D. d'Enterria, A. Dabrowski, A. David, A. De Roeck, M.M. Defranchis, M. Deile, M. Dobson, G. Franzoni, W. Funk, S. Giani, D. Gigi, K. Gill, F. Glege, J. Hegeman, J.K. Heikkilä, B. Huber, V. Innocente, T. James, P. Janot, O. Kaluzinska, O. Karacheban[28], S. Laurila, P. Lecoq, E. Leutgeb, C. Lourenço, L. Malgeri, M. Mannelli, M. Matthewman, A. Mehta, F. Meijers, S. Mersi, E. Meschi, V. Milosevic, F. Monti, F. Moortgat, M. Mulders, I. Neutelings, S. Orfanelli, F. Pantaleo, G. Petrucciani, A. Pfeiffer, M. Pierini, H. Qu, D. Rabady, B. Ribeiro Lopes, M. Rovere, H. Sakulin, S. Sanchez Cruz, S. Scarfi, C. Schwick, M. Selvaggi, A. Sharma, K. Shchelina, P. Silva, P. Sphicas[59], A.G. Stahl Leiton, A. Steen, S. Summers, D. Treille, P. Tropea, D. Walter, J. Wanczyk[60], J. Wang, S. Wuchterl, P. Zehetner, P. Zejdl, W.D. Zeuner

Paul Scherrer Institut, Villigen, Switzerland
T. Bevilacqua[61], L. Caminada[61], A. Ebrahimi, W. Erdmann, R. Horisberger, Q. Ingram, H.C. Kaestli, D. Kotlinski, C. Lange, M. Missiroli[61], L. Noehte[61], T. Rohe

ETH Zurich - Institute for Particle Physics and Astrophysics (IPA), Zurich, Switzerland
T.K. Aarrestad, K. Androsov[60], M. Backhaus, G. Bonomelli, A. Calandri, C. Cazzaniga, K. Datta, P. De Bryas Dexmiers D'archiac[60], A. De Cosa, G. Dissertori, M. Dittmar, M. Donegà, F. Eble, M. Galli, K. Gedia, F. Glessgen, C. Grab, N. Härringer, T.G. Harte, D. Hits, W. Lustermann, A.-M. Lyon, R.A. Manzoni, M. Marchegiani, L. Marchese, C. Martin Perez, A. Mascellani[60], F. Nessi-Tedaldi, F. Pauss, V. Perovic, S. Pigazzini, C. Reissel, B. Ristic, F. Riti, R. Seidita, J. Steggemann[60], A. Tarabini, D. Valsecchi, R. Wallny

Universität Zürich, Zurich, Switzerland
C. Amsler[62], P. Bärtschi, M.F. Canelli, K. Cormier, M. Huwiler, W. Jin, A. Jofrehei, B. Kilminster, S. Leontsinis, S.P. Liechti, A. Macchiolo, P. Meiring, F. Meng, U. Molinatti, J. Motta, A. Reimers, P. Robmann, M. Senger, E. Shokr, F. Stäger, R. Tramontano

National Central University, Chung-Li, Taiwan
C. Adloff[63], D. Bhowmik, C.M. Kuo, W. Lin, P.K. Rout, P.C. Tiwari[38], S.S. Yu

National Taiwan University (NTU), Taipei, Taiwan
L. Ceard, K.F. Chen, P.s. Chen, Z.g. Chen, A. De Iorio, W.-S. Hou, T.h. Hsu, Y.w. Kao, S. Karmakar, G. Kole, Y.y. Li, R.-S. Lu, E. Paganis, X.f. Su, J. Thomas-Wilsker, L.s. Tsai, D. Tsionou, H.y. Wu, E. Yazgan

High Energy Physics Research Unit, Department of Physics, Faculty of Science, Chulalongkorn University, Bangkok, Thailand
C. Asawatangtrakuldee, N. Srimanobhas, V. Wachirapusitanand

Çukurova University, Physics Department, Science and Art Faculty, Adana, Turkey
D. Agyel, F. Boran, F. Dolek, I. Dumanoglu[64], E. Eskut, Y. Guler[65], E. Gurpinar Guler[65], C. Isik, O. Kara, A. Kayis Topaksu, U. Kiminsu, G. Onengut, K. Ozdemir[66], A. Polatoz, B. Tali[67], U.G. Tok, S. Turkcapar, E. Uslan, I.S. Zorbakir

Middle East Technical University, Physics Department, Ankara, Turkey
G. Sokmen, M. Yalvac[68]

Bogazici University, Istanbul, Turkey
B. Akgun, I.O. Atakisi, E. Gülmez, M. Kaya[69], O. Kaya[70], S. Tekten[71]

Istanbul Technical University, Istanbul, Turkey
A. Cakir, K. Cankocak[64,72], G.G. Dincer[64], Y. Komurcu, S. Sen[73]

Istanbul University, Istanbul, Turkey
O. Aydilek[74], B. Hacisahinoglu, I. Hos[75], B. Kaynak, S. Ozkorucuklu, O. Potok, H. Sert, C. Simsek, C. Zorbilmez

Yildiz Technical University, Istanbul, Turkey
S. Cerci[67], B. Isildak[76], D. Sunar Cerci, T. Yetkin

Institute for Scintillation Materials of National Academy of Science of Ukraine, Kharkiv, Ukraine
A. Boyaryntsev, B. Grynyov

National Science Centre, Kharkiv Institute of Physics and Technology, Kharkiv, Ukraine
L. Levchuk

University of Bristol, Bristol, United Kingdom
D. Anthony, J.J. Brooke, A. Bundock, F. Bury, E. Clement, D. Cussans, H. Flacher, M. Glowacki, J. Goldstein, H.F. Heath, M.-L. Holmberg, L. Kreczko, S. Paramesvaran, L. Robertshaw, S. Seif El Nasr-Storey, V.J. Smith, N. Stylianou[77], K. Walkingshaw Pass

Rutherford Appleton Laboratory, Didcot, United Kingdom
A.H. Ball, K.W. Bell, A. Belyaev[78], C. Brew, R.M. Brown, D.J.A. Cockerill, C. Cooke, A. Elliot, K.V. Ellis, K. Harder, S. Harper, J. Linacre, K. Manolopoulos, D.M. Newbold, E. Olaiya, D. Petyt, T. Reis, A.R. Sahasransu, G. Salvi, T. Schuh, C.H. Shepherd-Themistocleous, I.R. Tomalin, K.C. Whalen, T. Williams

Imperial College, London, United Kingdom
I. Andreou, R. Bainbridge, P. Bloch, C.E. Brown, O. Buchmuller, V. Cacchio, C.A. Carrillo Montoya, G.S. Chahal[79], D. Colling, J.S. Dancu, I. Das, P. Dauncey, G. Davies, J. Davies, M. Della Negra, S. Fayer, G. Fedi, G. Hall, M.H. Hassanshahi, A. Howard, G. Iles, M. Knight, J. Langford, J. León Holgado, L. Lyons, A.-M. Magnan, S. Mallios, M. Mieskolainen, J. Nash[80], M. Pesaresi, P.B. Pradeep, B.C. Radburn-Smith, A. Richards, A. Rose, K. Savva, C. Seez, R. Shukla, A. Tapper, K. Uchida, G.P. Uttley, L.H. Vage, T. Virdee[30], M. Vojinovic, N. Wardle, D. Winterbottom

Brunel University, Uxbridge, United Kingdom
K. Coldham, J.E. Cole, A. Khan, P. Kyberd, I.D. Reid

Baylor University, Waco, Texas, USA
S. Abdullin, A. Brinkerhoff, E. Collins, J. Dittmann, K. Hatakeyama, J. Hiltbrand, B. McMaster, J. Samudio, S. Sawant, C. Sutantawibul, J. Wilson

Catholic University of America, Washington, DC, USA
R. Bartek, A. Dominguez, C. Huerta Escamilla, A.E. Simsek, R. Uniyal, A.M. Vargas Hernandez

The University of Alabama, Tuscaloosa, Alabama, USA
B. Bam, A. Buchot Perraguin, R. Chudasama, S.I. Cooper, C. Crovella, S.V. Gleyzer, E. Pearson, C.U. Perez, P. Rumerio[81], E. Usai, R. Yi

Boston University, Boston, Massachusetts, USA
A. Akpinar, C. Cosby, G. De Castro, Z. Demiragli, C. Erice, C. Fangmeier, C. Fernandez Madrazo, E. Fontanesi, D. Gastler, F. Golf, S. Jeon, J. O'cain, I. Reed, J. Rohlf, K. Salyer, D. Sperka, D. Spitzbart, I. Suarez, A. Tsatsos, A.G. Zecchinelli

Brown University, Providence, Rhode Island, USA
G. Benelli, D. Cutts, L. Gouskos, M. Hadley, U. Heintz, J.M. Hogan[82], T. Kwon, G. Landsberg, K.T. Lau, D. Li, J. Luo, S. Mondal, N. Pervan, T. Russell, S. Sagir[83], F. Simpson, M. Stamenkovic, N. Venkatasubramanian, X. Yan

University of California, Davis, Davis, California, USA
S. Abbott, C. Brainerd, R. Breedon, H. Cai, M. Calderon De La Barca Sanchez, M. Chertok, M. Citron, J. Conway, P.T. Cox, R. Erbacher, F. Jensen, O. Kukral, G. Mocellin, M. Mulhearn, S. Ostrom, W. Wei, Y. Yao, S. Yoo, F. Zhang

University of California, Los Angeles, California, USA

M. Bachtis, R. Cousins, A. Datta, G. Flores Avila, J. Hauser, M. Ignatenko, M.A. Iqbal, T. Lam, E. Manca, A. Nunez Del Prado, D. Saltzberg, V. Valuev

University of California, Riverside, Riverside, California, USA
R. Clare, J.W. Gary, M. Gordon, G. Hanson, W. Si

University of California, San Diego, La Jolla, California, USA
A. Aportela, A. Arora, J.G. Branson, S. Cittolin, S. Cooperstein, D. Diaz, J. Duarte, L. Giannini, Y. Gu, J. Guiang, R. Kansal, V. Krutelyov, R. Lee, J. Letts, M. Masciovecchio, F. Mokhtar, S. Mukherjee, M. Pieri, M. Quinnan, B.V. Sathia Narayanan, V. Sharma, M. Tadel, E. Vourliotis, F. Würthwein, Y. Xiang, A. Yagil

University of California, Santa Barbara - Department of Physics, Santa Barbara, California, USA
A. Barzdukas, L. Brennan, C. Campagnari, K. Downham, C. Grieco, J. Incandela, J. Kim, A.J. Li, P. Masterson, H. Mei, J. Richman, S.N. Santpur, U. Sarica, R. Schmitz, F. Setti, J. Sheplock, D. Stuart, T.Á. Vámi, S. Wang, D. Zhang

California Institute of Technology, Pasadena, California, USA
A. Bornheim, O. Cerri, A. Latorre, J. Mao, H.B. Newman, G. Reales Gutiérrez, M. Spiropulu, J.R. Vlimant, C. Wang, S. Xie, R.Y. Zhu

Carnegie Mellon University, Pittsburgh, Pennsylvania, USA
J. Alison, S. An, P. Bryant, M. Cremonesi, V. Dutta, T. Ferguson, T.A. Gómez Espinosa, A. Harilal, A. Kallil Tharayil, C. Liu, T. Mudholkar, S. Murthy, P. Palit, K. Park, M. Paulini, A. Roberts, A. Sanchez, W. Terrill

University of Colorado Boulder, Boulder, Colorado, USA
J.P. Cumalat, W.T. Ford, A. Hart, A. Hassani, G. Karathanasis, N. Manganelli, C. Savard, N. Schonbeck, K. Stenson, K.A. Ulmer, S.R. Wagner, N. Zipper, D. Zuolo

Cornell University, Ithaca, New York, USA
J. Alexander, S. Bright-Thonney, X. Chen, D.J. Cranshaw, J. Fan, X. Fan, S. Hogan, P. Kotamnives, J. Monroy, M. Oshiro, J.R. Patterson, M. Reid, A. Ryd, J. Thom, P. Wittich, R. Zou

Fermi National Accelerator Laboratory, Batavia, Illinois, USA
M. Albrow, M. Alyari, O. Amram, G. Apollinari, A. Apresyan, L.A.T. Bauerdick, D. Berry, J. Berryhill, P.C. Bhat, K. Burkett, J.N. Butler, A. Canepa, G.B. Cerati, H.W.K. Cheung, F. Chlebana, G. Cummings, J. Dickinson, I. Dutta, V.D. Elvira, Y. Feng, J. Freeman, A. Gandrakota, Z. Gecse, L. Gray, D. Green, A. Grummer, S. Grünendahl, D. Guerrero, O. Gutsche, R.M. Harris, R. Heller, T.C. Herwig, J. Hirschauer, B. Jayatilaka, S. Jindariani, M. Johnson, U. Joshi, T. Klijnsma, B. Klima, K.H.M. Kwok, S. Lammel, D. Lincoln, R. Lipton, T. Liu, C. Madrid, K. Maeshima, C. Mantilla, D. Mason, P. McBride, P. Merkel, S. Mrenna, S. Nahn, J. Ngadiuba, D. Noonan, S. Norberg, V. Papadimitriou, N. Pastika, K. Pedro, C. Pena[84], F. Ravera, A. Reinsvold Hall[85], L. Ristori, M. Safdari, E. Sexton-Kennedy, N. Smith, A. Soha, L. Spiegel, S. Stoynev, J. Strait, L. Taylor, S. Tkaczyk, N.V. Tran, L. Uplegger, E.W. Vaandering, I. Zoi

University of Florida, Gainesville, Florida, USA
C. Aruta, P. Avery, D. Bourilkov, P. Chang, V. Cherepanov, R.D. Field, E. Koenig,

M. Kolosova, J. Konigsberg, A. Korytov, K. Matchev, N. Menendez, G. Mitselmakher, K. Mohrman, A. Muthirakalayil Madhu, N. Rawal, S. Rosenzweig, Y. Takahashi, J. Wang

Florida State University, Tallahassee, Florida, USA
T. Adams, A. Al Kadhim, A. Askew, S. Bower, V. Hagopian, R. Hashmi, R.S. Kim, S. Kim, T. Kolberg, G. Martinez, H. Prosper, P.R. Prova, M. Wulansatiti, R. Yohay, J. Zhang

Florida Institute of Technology, Melbourne, Florida, USA
B. Alsufyani, M.M. Baarmand, S. Butalla, S. Das, T. Elkafrawy[86], M. Hohlmann, M. Rahmani, E. Yanes

University of Illinois Chicago, Chicago, USA, Chicago, USA
M.R. Adams, A. Baty, C. Bennett, R. Cavanaugh, R. Escobar Franco, O. Evdokimov, C.E. Gerber, M. Hawksworth, A. Hingrajiya, D.J. Hofman, J.h. Lee, D. S. Lemos, A.H. Merrit, C. Mills, S. Nanda, G. Oh, B. Ozek, D. Pilipovic, R. Pradhan, E. Prifti, T. Roy, S. Rudrabhatla, M.B. Tonjes, N. Varelas, M.A. Wadud, Z. Ye, J. Yoo

The University of Iowa, Iowa City, Iowa, USA
M. Alhusseini, D. Blend, K. Dilsiz[87], L. Emediato, G. Karaman, O.K. Köseyan, J.-P. Merlo, A. Mestvirishvili[88], O. Neogi, H. Ogul[89], Y. Onel, A. Penzo, C. Snyder, E. Tiras[90]

Johns Hopkins University, Baltimore, Maryland, USA
B. Blumenfeld, L. Corcodilos, J. Davis, A.V. Gritsan, L. Kang, S. Kyriacou, P. Maksimovic, M. Roguljic, J. Roskes, S. Sekhar, M. Swartz

The University of Kansas, Lawrence, Kansas, USA
A. Abreu, L.F. Alcerro Alcerro, J. Anguiano, S. Arteaga Escatel, P. Baringer, A. Bean, Z. Flowers, D. Grove, J. King, G. Krintiras, M. Lazarovits, C. Le Mahieu, J. Marquez, M. Murray, M. Nickel, M. Pitt, S. Popescu[91], C. Rogan, C. Royon, R. Salvatico, S. Sanders, C. Smith, G. Wilson

Kansas State University, Manhattan, Kansas, USA
B. Allmond, R. Gujju Gurunadha, A. Ivanov, K. Kaadze, Y. Maravin, J. Natoli, D. Roy, G. Sorrentino

University of Maryland, College Park, Maryland, USA
A. Baden, A. Belloni, J. Bistany-riebman, Y.M. Chen, S.C. Eno, N.J. Hadley, S. Jabeen, R.G. Kellogg, T. Koeth, B. Kronheim, Y. Lai, S. Lascio, A.C. Mignerey, S. Nabili, C. Palmer, C. Papageorgakis, M.M. Paranjpe, L. Wang

Massachusetts Institute of Technology, Cambridge, Massachusetts, USA
J. Bendavid, I.A. Cali, P.c. Chou, M. D'Alfonso, J. Eysermans, C. Freer, G. Gomez-Ceballos, M. Goncharov, G. Grosso, P. Harris, D. Hoang, D. Kovalskyi, J. Krupa, L. Lavezzo, Y.-J. Lee, K. Long, C. Mcginn, A. Novak, C. Paus, C. Roland, G. Roland, S. Rothman, G.S.F. Stephans, Z. Wang, B. Wyslouch, T. J. Yang

University of Minnesota, Minneapolis, Minnesota, USA
B. Crossman, B.M. Joshi, C. Kapsiak, M. Krohn, D. Mahon, J. Mans, B. Marzocchi, R. Rusack, R. Saradhy, N. Strobbe

University of Nebraska-Lincoln, Lincoln, Nebraska, USA
K. Bloom, D.R. Claes, G. Haza, J. Hossain, C. Joo, I. Kravchenko, J.E. Siado, W. Tabb, A. Vagnerini, A. Wightman, F. Yan, D. Yu

State University of New York at Buffalo, Buffalo, New York, USA
H. Bandyopadhyay, L. Hay, H.w. Hsia, I. Iashvili, A. Kalogeropoulos, A. Kharchilava, M. Morris, D. Nguyen, S. Rappoccio, H. Rejeb Sfar, A. Williams, P. Young

Northeastern University, Boston, Massachusetts, USA
G. Alverson, E. Barberis, J. Bonilla, J. Dervan, Y. Haddad, Y. Han, A. Krishna, J. Li, M. Lu, G. Madigan, R. Mccarthy, D.M. Morse, V. Nguyen, T. Orimoto, A. Parker, L. Skinnari, D. Wood

Northwestern University, Evanston, Illinois, USA
J. Bueghly, S. Dittmer, K.A. Hahn, Y. Liu, Y. Miao, D.G. Monk, M.H. Schmitt, A. Taliercio, M. Velasco

University of Notre Dame, Notre Dame, Indiana, USA
G. Agarwal, R. Band, R. Bucci, S. Castells, A. Das, R. Goldouzian, M. Hildreth, K.W. Ho, K. Hurtado Anampa, T. Ivanov, C. Jessop, K. Lannon, J. Lawrence, N. Loukas, L. Lutton, J. Mariano, N. Marinelli, I. Mcalister, T. McCauley, C. Mcgrady, C. Moore, Y. Musienko[17], H. Nelson, M. Osherson, A. Piccinelli, R. Ruchti, A. Townsend, Y. Wan, M. Wayne, H. Yockey, M. Zarucki, L. Zygala

The Ohio State University, Columbus, Ohio, USA
A. Basnet, B. Bylsma, M. Carrigan, L.S. Durkin, C. Hill, M. Joyce, M. Nunez Ornelas, K. Wei, B.L. Winer, B. R. Yates

Princeton University, Princeton, New Jersey, USA
H. Bouchamaoui, P. Das, G. Dezoort, P. Elmer, A. Frankenthal, B. Greenberg, N. Haubrich, K. Kennedy, G. Kopp, S. Kwan, D. Lange, A. Loeliger, D. Marlow, I. Ojalvo, J. Olsen, A. Shevelev, D. Stickland, C. Tully

University of Puerto Rico, Mayaguez, Puerto Rico, USA
S. Malik

Purdue University, West Lafayette, Indiana, USA
A.S. Bakshi, S. Chandra, R. Chawla, A. Gu, L. Gutay, M. Jones, A.W. Jung, A.M. Koshy, M. Liu, G. Negro, N. Neumeister, G. Paspalaki, S. Piperov, V. Scheurer, J.F. Schulte, M. Stojanovic, J. Thieman, A. K. Virdi, F. Wang, W. Xie

Purdue University Northwest, Hammond, Indiana, USA
J. Dolen, N. Parashar, A. Pathak

Rice University, Houston, Texas, USA
D. Acosta, T. Carnahan, K.M. Ecklund, P.J. Fernández Manteca, S. Freed, P. Gardner, F.J.M. Geurts, W. Li, J. Lin, O. Miguel Colin, B.P. Padley, R. Redjimi, J. Rotter, W. Shi, E. Yigitbasi, Y. Zhang

University of Rochester, Rochester, New York, USA
A. Bodek, P. de Barbaro, R. Demina, A. Garcia-Bellido, O. Hindrichs, A. Khukhunaishvili, N. Parmar, P. Parygin[92], E. Popova[92], R. Taus

Rutgers, The State University of New Jersey, Piscataway, New Jersey, USA

B. Chiarito, J.P. Chou, S.V. Clark, D. Gadkari, Y. Gershtein, E. Halkiadakis, M. Heindl, C. Houghton, D. Jaroslawski, S. Konstantinou, I. Laflotte, A. Lath, R. Montalvo, K. Nash, J. Reichert, H. Routray, P. Saha, S. Salur, S. Schnetzer, S. Somalwar, R. Stone, S.A. Thayil, S. Thomas, J. Vora, H. Wang

University of Tennessee, Knoxville, Tennessee, USA
D. Ally, A.G. Delannoy, S. Fiorendi, S. Higginbotham, T. Holmes, A.R. Kanuganti, N. Karunarathna, L. Lee, E. Nibigira, S. Spanier

Texas A&M University, College Station, Texas, USA
D. Aebi, M. Ahmad, T. Akhter, O. Bouhali[93], R. Eusebi, J. Gilmore, T. Huang, T. Kamon[94], H. Kim, S. Luo, R. Mueller, D. Overton, D. Rathjens, A. Safonov

Texas Tech University, Lubbock, Texas, USA
N. Akchurin, J. Damgov, N. Gogate, V. Hegde, A. Hussain, Y. Kazhykarim, K. Lamichhane, S.W. Lee, A. Mankel, T. Peltola, I. Volobouev

Vanderbilt University, Nashville, Tennessee, USA
E. Appelt, Y. Chen, S. Greene, A. Gurrola, W. Johns, R. Kunnawalkam Elayavalli, A. Melo, F. Romeo, P. Sheldon, S. Tuo, J. Velkovska, J. Viinikainen

University of Virginia, Charlottesville, Virginia, USA
B. Cardwell, B. Cox, J. Hakala, R. Hirosky, A. Ledovskoy, C. Neu

Wayne State University, Detroit, Michigan, USA
S. Bhattacharya, P.E. Karchin

University of Wisconsin - Madison, Madison, Wisconsin, USA
A. Aravind, S. Banerjee, K. Black, T. Bose, S. Dasu, I. De Bruyn, P. Everaerts, C. Galloni, H. He, M. Herndon, A. Herve, C.K. Koraka, A. Lanaro, R. Loveless, J. Madhusudanan Sreekala, A. Mallampalli, A. Mohammadi, S. Mondal, G. Parida, L. Pétré, D. Pinna, A. Savin, V. Shang, V. Sharma, W.H. Smith, D. Teague, H.F. Tsoi, W. Vetens, A. Warden

Authors affiliated with an institute or an international laboratory covered by a cooperation agreement with CERN
S. Afanasiev, V. Alexakhin, D. Budkouski, I. Golutvin†, I. Gorbunov, V. Karjavine, V. Korenkov, A. Lanev, A. Malakhov, V. Matveev[95], V. Palichik, V. Perelygin, M. Savina, V. Shalaev, S. Shmatov, S. Shulha, V. Smirnov, O. Teryaev, N. Voytishin, B.S. Yuldashev[96], A. Zarubin, I. Zhizhin, G. Gavrilov, V. Golovtcov, Y. Ivanov, V. Kim[95], P. Levchenko[97], V. Murzin, V. Oreshkin, D. Sosnov, V. Sulimov, L. Uvarov, A. Vorobyev†, Yu. Andreev, A. Dermenev, S. Gninenko, N. Golubev, A. Karneyeu, D. Kirpichnikov, M. Kirsanov, N. Krasnikov, I. Tlisova, A. Toropin, T. Aushev, V. Gavrilov, N. Lychkovskaya, A. Nikitenko[98,99], V. Popov, A. Zhokin, M. Chadeeva[95], R. Chistov[95], S. Polikarpov[95], V. Andreev, M. Azarkin, M. Kirakosyan, A. Terkulov, E. Boos, V. Bunichev, M. Dubinin[84], L. Dudko, A. Gribushin, V. Klyukhin, O. Kodolova[99], S. Obraztsov, M. Perfilov, S. Petrushanko, V. Savrin, G. Vorotnikov, V. Blinov[95], T. Dimova[95], A. Kozyrev[95], O. Radchenko[95], Y. Skovpen[95], V. Kachanov, D. Konstantinov, S. Slabospitskii, A. Uzunian, A. Babaev, V. Borshch, D. Druzhkin[100]

Authors affiliated with an institute formerly covered by a cooperation agreement with CERN
V. Chekhovsky, V. Makarenko

†: Deceased
[1]Also at Yerevan State University, Yerevan, Armenia
[2]Also at TU Wien, Vienna, Austria
[3]Also at Institute of Basic and Applied Sciences, Faculty of Engineering, Arab Academy for Science, Technology and Maritime Transport, Alexandria, Egypt
[4]Also at Ghent University, Ghent, Belgium
[5]Also at Universidade do Estado do Rio de Janeiro, Rio de Janeiro, Brazil
[6]Also at Universidade Estadual de Campinas, Campinas, Brazil
[7]Also at Federal University of Rio Grande do Sul, Porto Alegre, Brazil
[8]Also at UFMS, Nova Andradina, Brazil
[9]Also at Nanjing Normal University, Nanjing, China
[10]Now at The University of Iowa, Iowa City, Iowa, USA
[11]Also at University of Chinese Academy of Sciences, Beijing, China
[12]Also at China Center of Advanced Science and Technology, Beijing, China
[13]Also at University of Chinese Academy of Sciences, Beijing, China
[14]Also at China Spallation Neutron Source, Guangdong, China
[15]Now at Henan Normal University, Xinxiang, China
[16]Also at Université Libre de Bruxelles, Bruxelles, Belgium
[17]Also at an institute or an international laboratory covered by a cooperation agreement with CERN
[18]Also at Suez University, Suez, Egypt
[19]Now at British University in Egypt, Cairo, Egypt
[20]Also at Purdue University, West Lafayette, Indiana, USA
[21]Also at Université de Haute Alsace, Mulhouse, France
[22]Also at Istinye University, Istanbul, Turkey
[23]Also at Ilia State University, Tbilisi, Georgia
[24]Also at The University of the State of Amazonas, Manaus, Brazil
[25]Also at University of Hamburg, Hamburg, Germany
[26]Also at RWTH Aachen University, III. Physikalisches Institut A, Aachen, Germany
[27]Also at Bergische University Wuppertal (BUW), Wuppertal, Germany
[28]Also at Brandenburg University of Technology, Cottbus, Germany
[29]Also at Forschungszentrum Jülich, Juelich, Germany
[30]Also at CERN, European Organization for Nuclear Research, Geneva, Switzerland
[31]Also at Institute of Nuclear Research ATOMKI, Debrecen, Hungary
[32]Now at Universitatea Babes-Bolyai - Facultatea de Fizica, Cluj-Napoca, Romania
[33]Also at MTA-ELTE Lendület CMS Particle and Nuclear Physics Group, Eötvös Loránd University, Budapest, Hungary
[34]Also at HUN-REN Wigner Research Centre for Physics, Budapest, Hungary
[35]Also at Physics Department, Faculty of Science, Assiut University, Assiut, Egypt
[36]Also at Punjab Agricultural University, Ludhiana, India
[37]Also at University of Visva-Bharati, Santiniketan, India
[38]Also at Indian Institute of Science (IISc), Bangalore, India
[39]Also at IIT Bhubaneswar, Bhubaneswar, India
[40]Also at Institute of Physics, Bhubaneswar, India
[41]Also at University of Hyderabad, Hyderabad, India
[42]Also at Deutsches Elektronen-Synchrotron, Hamburg, Germany
[43]Also at Isfahan University of Technology, Isfahan, Iran
[44]Also at Sharif University of Technology, Tehran, Iran
[45]Also at Department of Physics, University of Science and Technology of Mazandaran,

Behshahr, Iran
[46]Also at Department of Physics, Isfahan University of Technology, Isfahan, Iran
[47]Also at Department of Physics, Faculty of Science, Arak University, ARAK, Iran
[48]Also at Helwan University, Cairo, Egypt
[49]Also at Italian National Agency for New Technologies, Energy and Sustainable Economic Development, Bologna, Italy
[50]Also at Centro Siciliano di Fisica Nucleare e di Struttura Della Materia, Catania, Italy
[51]Also at Università degli Studi Guglielmo Marconi, Roma, Italy
[52]Also at Scuola Superiore Meridionale, Università di Napoli 'Federico II', Napoli, Italy
[53]Also at Fermi National Accelerator Laboratory, Batavia, Illinois, USA
[54]Also at Consiglio Nazionale delle Ricerche - Istituto Officina dei Materiali, Perugia, Italy
[55]Also at Department of Applied Physics, Faculty of Science and Technology, Universiti Kebangsaan Malaysia, Bangi, Malaysia
[56]Also at Consejo Nacional de Ciencia y Tecnología, Mexico City, Mexico
[57]Also at Trincomalee Campus, Eastern University, Sri Lanka, Nilaveli, Sri Lanka
[58]Also at Saegis Campus, Nugegoda, Sri Lanka
[59]Also at National and Kapodistrian University of Athens, Athens, Greece
[60]Also at Ecole Polytechnique Fédérale Lausanne, Lausanne, Switzerland
[61]Also at Universität Zürich, Zurich, Switzerland
[62]Also at Stefan Meyer Institute for Subatomic Physics, Vienna, Austria
[63]Also at Laboratoire d'Annecy-le-Vieux de Physique des Particules, IN2P3-CNRS, Annecy-le-Vieux, France
[64]Also at Near East University, Research Center of Experimental Health Science, Mersin, Turkey
[65]Also at Konya Technical University, Konya, Turkey
[66]Also at Izmir Bakircay University, Izmir, Turkey
[67]Also at Adiyaman University, Adiyaman, Turkey
[68]Also at Bozok Universitetesi Rektörlügü, Yozgat, Turkey
[69]Also at Marmara University, Istanbul, Turkey
[70]Also at Milli Savunma University, Istanbul, Turkey
[71]Also at Kafkas University, Kars, Turkey
[72]Now at Istanbul Okan University, Istanbul, Turkey
[73]Also at Hacettepe University, Ankara, Turkey
[74]Also at Erzincan Binali Yildirim University, Erzincan, Turkey
[75]Also at Istanbul University - Cerrahpasa, Faculty of Engineering, Istanbul, Turkey
[76]Also at Yildiz Technical University, Istanbul, Turkey
[77]Also at Vrije Universiteit Brussel, Brussel, Belgium
[78]Also at School of Physics and Astronomy, University of Southampton, Southampton, United Kingdom
[79]Also at IPPP Durham University, Durham, United Kingdom
[80]Also at Monash University, Faculty of Science, Clayton, Australia
[81]Also at Università di Torino, Torino, Italy
[82]Also at Bethel University, St. Paul, Minnesota, USA
[83]Also at Karamanoğlu Mehmetbey University, Karaman, Turkey
[84]Also at California Institute of Technology, Pasadena, California, USA
[85]Also at United States Naval Academy, Annapolis, Maryland, USA
[86]Also at Ain Shams University, Cairo, Egypt
[87]Also at Bingol University, Bingol, Turkey
[88]Also at Georgian Technical University, Tbilisi, Georgia

[89]Also at Sinop University, Sinop, Turkey
[90]Also at Erciyes University, Kayseri, Turkey
[91]Also at Horia Hulubei National Institute of Physics and Nuclear Engineering (IFIN-HH), Bucharest, Romania
[92]Now at another institute or international laboratory covered by a cooperation agreement with CERN
[93]Also at Texas A&M University at Qatar, Doha, Qatar
[94]Also at Kyungpook National University, Daegu, Korea
[95]Also at another institute or international laboratory covered by a cooperation agreement with CERN
[96]Also at Institute of Nuclear Physics of the Uzbekistan Academy of Sciences, Tashkent, Uzbekistan
[97]Also at Northeastern University, Boston, Massachusetts, USA
[98]Also at Imperial College, London, United Kingdom
[99]Now at Yerevan Physics Institute, Yerevan, Armenia
[100]Also at Universiteit Antwerpen, Antwerpen, Belgium